

Phase behavior and properties of the liquid-crystal dimer 1'',7''-bis(4-cyanobiphenyl-4'-yl) heptane: A twist-bend nematic liquid crystal

M. Cestari,^{1,2} S. Diez-Berart,³ D. A. Dunmur,^{1,*} A. Ferrarini,² M. R. de la Fuente,⁴ D. J. B. Jackson,¹ D. O. Lopez,³ G. R. Luckhurst,¹ M. A. Perez-Jubindo,⁴ R. M. Richardson,⁵ J. Salud,³ B. A. Timimi,¹ and H. Zimmermann⁶

¹*School of Chemistry, University of Southampton, Southampton SO17 1BJ, United Kingdom*

²*Department of Chemical Science, University of Padua, I-35131 Padua, Italy*

³*Department of Physics and Nuclear Engineering, Polytechnic University of Catalonia, Barcelona, Spain*

⁴*Department of Applied Physics II, University of the Basque Country, E-48080 Bilbao, Spain*

⁵*H. H. Wills Physics Laboratory, University of Bristol, Bristol BS8 1TL, United Kingdom*

⁶*Department of Biophysics, Max-Planck-Institut für Medizinische Forschung, D-69120 Heidelberg, Germany*

(Received 3 March 2011; revised manuscript received 17 May 2011; published 16 September 2011)

The liquid-crystal dimer 1'',7''-bis(4-cyanobiphenyl-4'-yl)heptane (CB7CB) exhibits two liquid-crystalline mesophases on cooling from the isotropic phase. The high-temperature phase is nematic; the identification and characterization of the other liquid-crystal phase is reported in this paper. It is concluded that the low-temperature mesophase of CB7CB is a new type of uniaxial nematic phase having a nonuniform director distribution composed of twist-bend deformations. The techniques of small-angle x-ray scattering, modulated differential scanning calorimetry, and dielectric spectroscopy have been applied to establish the nature of the nematic-nematic phase transition and the structural features of the twist-bend nematic phase. In addition, magnetic resonance studies (electron-spin resonance and ²H nuclear magnetic resonance) have been used to investigate the orientational order and director distribution in the liquid-crystalline phases of CB7CB. The synthesis of a specifically deuterated sample of CB7CB is reported, and measurements showed a bifurcation of the quadrupolar splitting on entering the low-temperature mesophase from the high-temperature nematic phase. This splitting could be interpreted in terms of the chirality of the twist-bend structure of the director. Calculations using an atomistic model and the surface interaction potential with Monte Carlo sampling have been carried out to determine the conformational distribution and predict dielectric and elastic properties in the nematic phase. The former are in agreement with experimental measurements, while the latter are consistent with the formation of a twist-bend nematic phase.

DOI: [10.1103/PhysRevE.84.031704](https://doi.org/10.1103/PhysRevE.84.031704)

PACS number(s): 61.30.Cz, 77.84.Nh, 64.70.M–, 61.30.Eb

I. INTRODUCTION

Liquid crystals will only form if the constituent molecules, macromolecules, or clusters of molecules possess shape anisotropy. Molecular shape influences the packing of molecules through their excluded volume, but shape also determines the longer-range attractive and repulsive forces responsible for the stability of liquid-crystal phases. The importance of shape in determining the phase behavior of liquid crystals has long been recognized [1,2], and there have been many studies on the corresponding relationships between molecular structure and mesophase properties. Thus, there is a hierarchy of phases of different symmetries that are formed from rod-shaped molecules, a different hierarchy for disk-shaped molecules, and yet another set of phases (so-called banana phases) for V-shaped or bent core molecules. Of course, there are overlaps between the phase types formed by the different classes of molecular shapes, e.g., rod-shaped, disk-shaped, and V-shaped molecules can all form nematic phases, but it is the particular molecular shape that determines the sequence of liquid-crystal phases for a class of compounds.

Although shape is of over-riding importance, the details of the molecular structure also strongly influence the phase behavior and properties of liquid crystals. Next to shape, molecular flexibility is probably the most important structural feature of a mesogen [a compound that can form a liquid-

crystal (meso)phase]. If the flexible part of a molecule is located in its core, then flexibility can significantly alter the shape of the molecule, and hence can have a profound effect on the phase behavior and properties. Mesogens having flexibility in the core occur in many guises, and again have been much studied for their liquid-crystal behavior. Side-chain and main-chain liquid-crystal polymers [3] have internal flexible linkages as an intrinsic part of their structure. Dendrimers [4] and multipodes [5] have flexible linking chains as part of three-dimensional (3D) macromolecular structures that can also form liquid-crystal phases. The simplest molecular structure having core flexibility is a dimer structure in which two semirigid mesogenic groups are connected by a flexible chain. Liquid-crystal dimers have attracted considerable attention in recent years [6], and this paper presents an extensive study of a deceptively simple symmetric dimer 1'',7''-bis(4-cyanobiphenyl-4'-yl)heptane (CB7CB), see Fig. 1.

The phase behavior of liquid-crystal dimers depends strongly on the nature of the flexible linking chain, and for a given species of chain the important properties are the chain length, as determined by the number of linking groups, and the parity of the chain, i.e., even or odd numbers of linking groups. For very short chains, the orientations of the two mesogenic groups are strongly coupled, and the dimer behaves more like a rigid molecule. For long chains, the mesogenic groups become more independent, and some properties of the mesophases are more similar to the properties of phases consisting of the monomeric forms of the mesogenic groups. Many properties of the mesophases of liquid-crystal

*d.dunmur@tiscali.co.uk

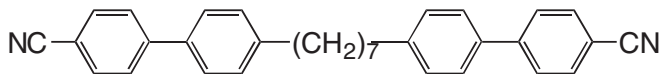


FIG. 1. Schematic chemical structure of the mesogenic dimer 1'',7''-bis(4-cyanobiphenyl-4'-yl)heptane (CB7CB).

dimers exhibit an odd-even effect reflecting the parity of the chain. Thus mesogens with an even-parity chain have higher mesophase transition temperatures and transitional entropies than the corresponding mesogens with odd-parity chains adjacent to them in the homologous series [7]. This odd-even effect is well-explained by a number of theories [8], which take into account the different anisotropic shapes of conformers allowed for odd- or even-membered chains. The energetically favored molecular shapes (conformers) are different for odd- and even-parity dimers, and the distribution of conformers between the accessible states can change with temperature over the range of the mesophase. It is expected that the different conformational distributions of odd and even dimers will have a significant effect on certain of their physical properties.

One property that is particularly sensitive to changes in molecular shape is the electric permittivity [9]. Assuming that molecules contain dipolar groups, then the dielectric response is a measure of the mean-square dipole moment of the molecule or groups of molecules interacting in the macroscopic environment. The mean-square dipole moment is an averaged vector sum of the constituent dipoles, which may have differing orientations within the molecule, and this vector sum is directly related to the molecular shape or conformation. For liquid crystals, the electric permittivity is a directional property, having two independently measurable components for uniaxial phases. These quantities, parallel and perpendicular to the director, provide a measure of the mean-square dipole moment along and perpendicular to the alignment axis of the liquid crystal. Dielectric measurements are usually made over a range of frequencies. The measurements of absorptions (dielectric losses) as a function of frequency provide further information on the rotational dynamics of the dipolar groups of the molecule. Our published data on the dielectric properties of symmetric and nonsymmetric dimers [10] have required the development of new theoretical models to explain the results [11].

There is a current interest in bent or V-shaped molecules, which pose new challenges to our understanding of liquid-crystal behavior. These molecules are intermediate in shape between calamitic (rodlike) and discotic (disklike) molecules, and the mesophases they exhibit are also intermediate in structure between the phase types characteristic of rodlike and disklike molecules. The new structures have been characterized as *B* (banana) phases, though in many cases there are similarities with known calamitic and columnar phases. It seems that the elusive biaxial nematic liquid crystal is one mesophase exhibited by certain bent core molecules [12], but other work indicates that different nematic phases, as yet unidentified, may also result from bent molecules [13–17].

The synthesis of the liquid-crystal dimer CB7CB has been previously reported [18]; in this work, its mesophase behavior is examined using a wide range of techniques. Optical microscopy has revealed the existence of two liquid-crystalline phases, namely a high-temperature nematic phase and a

low-temperature mesophase. This behavior is unexpected since the structurally similar α,ω -bis(4-cyanobiphenyl-4'-yloxy)alkanes only exhibit nematic phases and no other liquid-crystal phases [19]. The identification of the low-temperature liquid-crystal phase of CB7CB forms the major part of this investigation.

The structure of the paper is as follows. First, the synthesis of specifically deuterated CB7CB for deuterium nuclear magnetic resonance (NMR) experiments is given. The initial characterization of the mesophase properties of the dimer CB7CB is then described, along with transition temperatures, enthalpies of transition, and optical textures. Results of measurements of heat capacity and frequency-dependent dielectric permittivities as a function of temperature are reported. These are macroscopic properties, though the dielectric properties can be interpreted in terms of molecular theories. Electron-spin resonance (ESR) measurements on a nitroxide spin probe dissolved in CB7CB and NMR experiments on a deuterated sample of CB7CB are described. Model calculations of the conformational distributions of CB7CB in the nematic mesophase are reported, and they provide a theoretical basis for the interpretation of the other property measurements. Finally, the collected results from all techniques are discussed together, and a model for the structure and organization of the low-temperature liquid-crystal phase of CB7CB is proposed. This study is perhaps the most comprehensive ever reported in a single paper for a single mesogenic compound. The conclusions include a model for the liquid-crystal properties of CB7CB, but also have profound implications for the molecular organization and properties of liquid-crystal phases composed of sufficiently bent molecules.

II. SYNTHESIS AND LIQUID-CRYSTAL PHASE BEHAVIOR

The synthesis of CB7CB has been reported earlier [18], but for the purposes of this investigation, specifically deuterated CB7CB-*d*₄ was also required. The preparation followed the reported reaction scheme with the exception of the step to introduce the deuterons into the end positions of the heptyl chain via the reduction of 1'',7''-bis(4-bromobiphenyl-4'-carbonyl)pentane to 1'',7''-bis(4-bromobiphenyl-4'-yl)heptane-1'',7''-*d*₄. For this, a slurry of AlCl₃ (17.7 g) and LiAlD₄ (2.8 g) in dry diethyl ether (400 ml) was diluted with CDCl₃ (200 ml) and stirred for 1 h at 0 °C. To this slurry was added slowly solid 1'',7''-bis(4-bromobiphenyl-4'-carbonyl)pentane (6 g) and the reaction was warmed to room temperature and stirred for 16 h. The mixture was quenched with water (100 ml) and neutralized with HCl (1 M). The aqueous layer was extracted using DCM (3 × 50 ml) and the organics combined and dried over anhydrous MgSO₄. The solvents were removed *in vacuo* and the crude product purified by column chromatography (50% pet ether/DCM) to yield a white crystalline solid. The cyanation to give CB7CB-*d*₄ was performed as described previously [18]. The product was purified by chromatography (silica, DCM) followed by recrystallization from toluene/*n*-hexane. NMR and mass spectroscopy gave an empirical formula C₃₃H₂₆D₄N₂, *m/z* = 458 (100%), which showed a deuteration ≥ 98%.

Transition temperatures for hydrogenated CB7CB were determined using a polarizing microscope (Olympus Universal Microscope) fitted with a Linkham hot-stage. Differential scanning calorimetry (Perkin Elmer DSC7) was used to determine the enthalpies of transition. Two liquid-crystal phases were observed on cooling from the isotropic phase. At $T_{NI} = 116 \pm 1$ °C, a characteristic nematic phase was formed, the transitional entropy for which was determined as $\Delta S_{NI}/R = 0.34$. Further cooling revealed a low-temperature mesophase at $T_{XN} = 103 \pm 1$ °C. For the moment, we designate this as an unknown (*X*) phase, and much of the work described in this paper was directed to determining, unequivocally, the nature of this phase. The corresponding entropy of transition was determined as $\Delta S_{XN}/R = 0.31$. Thus both transitions can be described as weakly first order, and microscopic observations indicated a two-phase coexistence region at each transition of approximately 0.1 °C. The low-temperature liquid-crystal (*X*) phase supercooled extensively; the crystalline form of CB7CB melted on heating at 102 °C. The transitional properties are in keeping with those observed originally [18]. We should also note that in the original study, the *X* phase was tentatively identified as a smectic *A*, but our far more detailed investigations reported here have shown this to be incorrect.

The nematic phase of CB7CB was clearly identified from the Schlieren texture that formed readily in suitable thin-film samples, observed under the polarizing microscope. Identification of the low-temperature *X* phase was less certain. Different optical textures could be generated depending on sample preparation and thermal history. The most characteristic texture of the *X* phase of CB7CB was a broken focal conic fan texture [see Fig. 2(a)], typical of tilted smectic phases. This readily formed in thin samples without surface treatment, and also in samples with planar surface alignment. With thin samples contained between untreated cover slips, it was possible to observe a texture of elongated ellipses, often seen with antiferroelectric liquid crystals [see Fig. 2(b)]. In Fig. 2(b), a striped structure is visible that becomes more pronounced in cells with surface treatment.

Other textures presented in Fig. 2 reveal some features of the *X* phase. The formation of focal conics indicates that there is an optical periodicity in the phase, though the focal conics are truncated. In cells with a defined planar alignment direction for the low-temperature *X* phase, a characteristic striped texture develops with the stripes parallel to the surface alignment direction. These stripes exhibit a periodicity perpendicular to the stripe direction, of the order of a few microns, the contrast of which is maximized by rotation of the microscope stage by approximately $\pm 10^\circ$. The precise amount of rotation depends on the temperature. Careful examination of the striped texture also reveals tilted bands across the stripes, which prompts us to call the texture a rope texture.

The optical birefringence colors of consecutive stripes reverse on rotation by $\pm 10^\circ$, which suggests that domains have formed in the liquid-crystal film having equal, but opposite, optical birefringence. This would be consistent with the formation of chiral domains of opposite handedness. Distorted regions of the rope texture [see Figs. 2(e) and 2(f)] exhibit tilted ellipses that resemble the polygon texture associated

with focal conic structures. On further cooling, the ropelike texture reverts to the broken fan texture.

Similar textures to those presented in Fig. 2 have been published for other symmetric dimeric molecules [14,17] in the low-temperature phase following an apparent nematic-nematic phase transition.

Under some conditions, including the application of an electric field across the cell [see Figs. 9(a)–9(c)], samples of the *X* phase formed homeotropic textures, i.e., the optical image was dark and unchanged on rotation of the sample between crossed polarizers. This observation strongly suggests that the phase was not tilted, though this would not exclude structures having local molecular tilt uniformly distributed in the plane orthogonal to the director.

III. X-RAY SCATTERING STUDIES OF THE LIQUID-CRYSTAL PHASES OF CB7CB

Scattering images of x-rays (Cu $K\alpha$ radiation with a Ni filter and a graphite monochromator) from CB7CB were obtained in the nematic and low-temperature liquid-crystalline phases. The 2D image from the aligned nematic phase exhibited the characteristic pattern of diffuse inner and outer arcs corresponding to short-range intermolecular correlations along and perpendicular to the aligning magnetic field of approximately 1 T.

To obtain the images in the low-temperature phase, the sample was cooled from 115 °C (T_{NI}) to 86 °C in the presence of a 1 T horizontal magnetic field. The scattering pattern shown in Fig. 3(a) was obtained with the x-ray beam perpendicular to the director axis determined by the magnetic field. Then with the field removed, the sample was rotated by 90° so that the director was now parallel to the x-ray beam and the scattering pattern shown in Fig. 3(b) was obtained. The field was removed to prevent the realignment of the director following sample rotation.

The scattering patterns obtained from both the nematic and the unknown *X* phase were similar. The inner and outer diffuse rings in the low-temperature *X* phase are slightly broader than in the nematic phase, suggesting some additional disorder, but there is no hint of any splitting in the outer arcs, which would be expected if a tilt had developed. Also, there is no sign of a sharp layer reflection, which would indicate a smectic phase. When viewed along the director axis, the scattering pattern [Fig. 3(b)] has circular symmetry, suggesting that the sample has uniaxial symmetry in keeping with the symmetry of the aligning field.

The azimuthally averaged scattering intensity obtained from Fig. 3(b) is shown as a function of the scattering vector, Q , in Fig. 4. Two diffuse peaks are observed, the outer one corresponding to an average separation ($=2\pi/Q$) of 4.5 Å, which is typical for most rodlike liquid crystals. The inner, diffuse peak corresponds to a repeat distance of 12 Å. The molecular length of CB7CB was found to be 26 Å from both quantum-mechanical calculations and the x-ray crystal structure determination (see the supplemental material [61]). Accordingly, the x-ray scattering from the *X* phase suggests an intercalated structure. We note that the scattering pattern for the high-temperature nematic phase indicates that this also

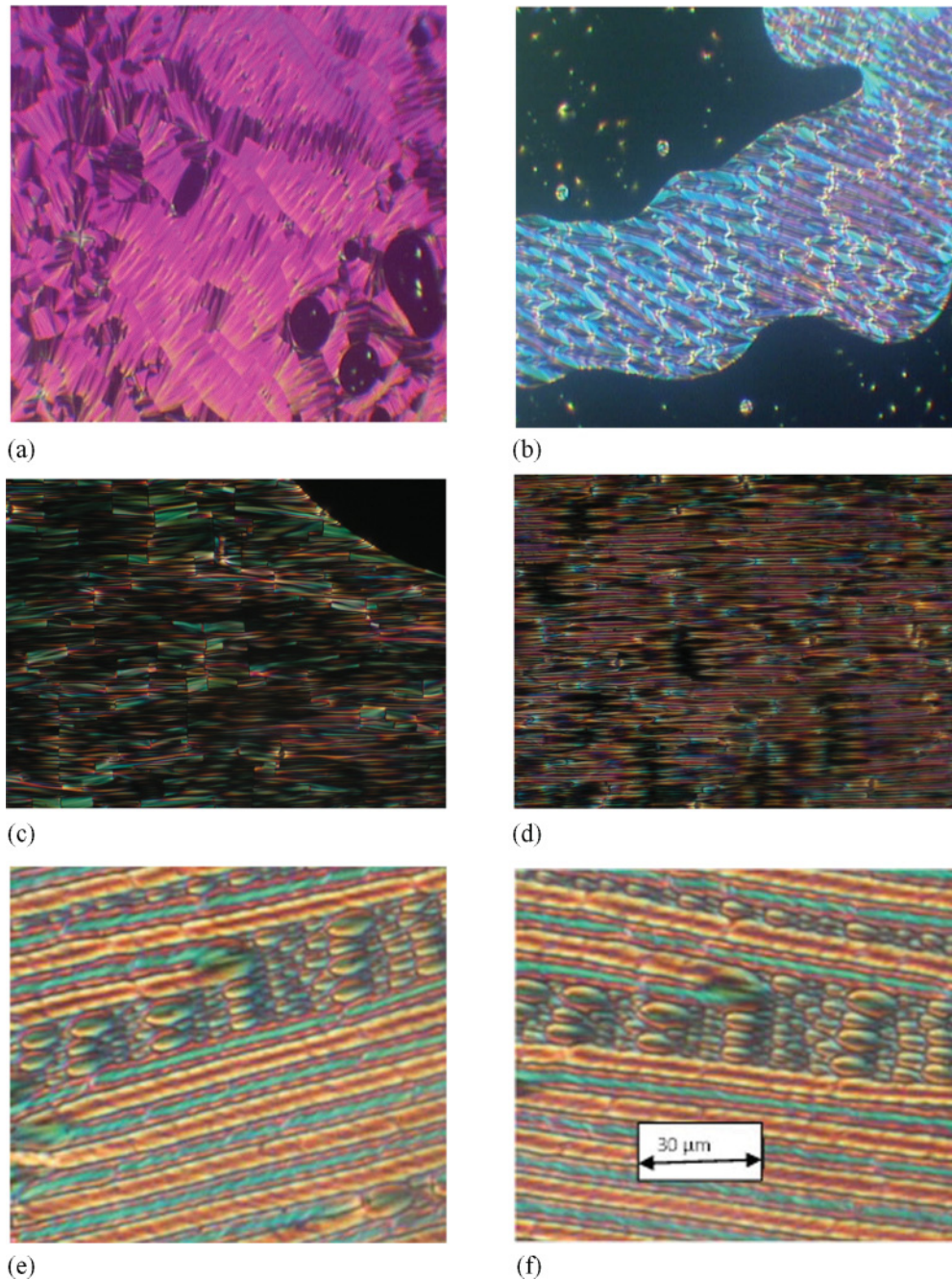


FIG. 2. (Color) (a) The broken fan texture formed in thin cells without surface treatment. (b) A texture of extended ellipses and hyperbolas reminiscent of antiferroelectric smectic-*C* phases. Textures in (c)–(f) are formed in cells with uniform planar surface alignment. The texture in (c) forms at the transition (103 °C) to the low-temperature *X* phase. On cooling, this rapidly changes into the texture (d) showing elongated ellipses to the left and right. Parts (e) and (f) show the characteristic striped texture (100.5 °C) at higher magnification with the stage rotated counterclockwise (e) by 10° and clockwise (f) by 10°: the white rectangle provides a scale. The polarizer axes are parallel to the edges of the photomicrographs.

has an intercalated structure. Fitting the inner diffuse peak in Fig. 4 to a Lorentzian function gives a correlation length of 17 Å, consistent with an intercalated nematic phase having a translational correlation distance of about one molecule along the director. We shall, therefore, denote this as an N_X phase from now on.

The conclusion from these studies is that the low-temperature phase is not a conventional smectic phase, as was first thought [18], and that any tendency to layer formation

is extremely weak; it is more correctly described as an intercalated nematic phase.

IV. MODULATED DIFFERENTIAL SCANNING CALORIMETRY OF THE N_X -*N* TRANSITION

The technique of modulated differential scanning calorimetry [20–22] enables the heat capacity of a material to be measured with very high precision as a function of temperature

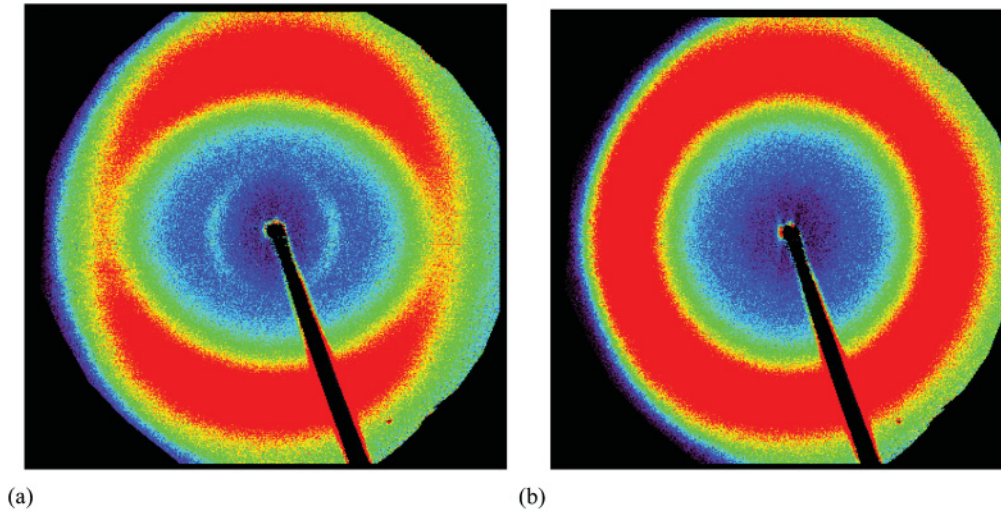


FIG. 3. (Color) X-ray scattering images from a magnetically aligned sample of CB7CB in the supercooled X phase at 86°C . The incident x-ray beam is perpendicular to the page. Part (a) is with the field in the plane of the page, and (b) is with the sample rotated so that the original field direction is perpendicular to the page.

in the region of a phase transition. A tricritical point associated with mesophase transitions is the temperature at which a first-order transition becomes a continuous or second-order transition [23]. This change from first order to second order occurs because of the coupling between two order parameters, which in the case of a nematic-to-smectic transition are the orientational order parameter and a translational order parameter, which describes the amplitude of a density wave associated with the smectic layers. Of course, the phenomenological theory that describes the tricritical behavior does not define the nature of the order parameters, only that there should be two and that they should couple in some way.

The results obtained for the heat capacity of CB7CB in the vicinity of the N_X - N phase transition are given in Fig. 5. Following the mean-field Landau model for second-order transitions, the excess heat capacity in the N_X phase ΔC_p (see the inset of Fig. 5) close to the N_X - N transition can be fitted by the expression

$$\Delta C_p = A^*(T_K - T)^{-1/2}. \quad (1)$$

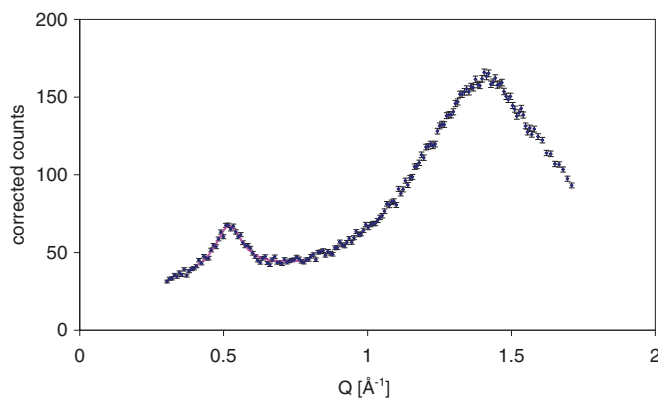


FIG. 4. (Color online) The azimuthally averaged scattering intensity determined for CB7CB in the aligned X phase at 86°C as a function of the scattering vector, Q .

The fitting parameters A^* and T_K are related to the Landau free-energy density coefficients ($g = g_0 + a[(T/T_0) - 1]\psi^2 + c\psi^4 + e\psi^{6+} \dots$, where ψ is the defining scalar order parameter of the N_X phase and g_0 is the free-energy density in the N phase) as

$$A^* = \left(\frac{a^3}{12eT_0} \right), \quad T_K = \left[1 + \frac{c^2}{3ae} \right] T_0; \quad (2)$$

the quantity T_0 is a hypothetical tricritical temperature.

The key result from our measurements is a value for (c^2/ae) of 0.0045, which gives $T_K/T_0 = 1.0015$; we note that a value of $T_K/T_1 = 1$ corresponds to a tricritical transition. This suggests that the transition observed in CB7CB between the N_X phase and the nematic phase is very close to being tricritical, although this does not help to confirm the low-temperature phase as a nematic. From the heat capacity results for the N_X - N transition,

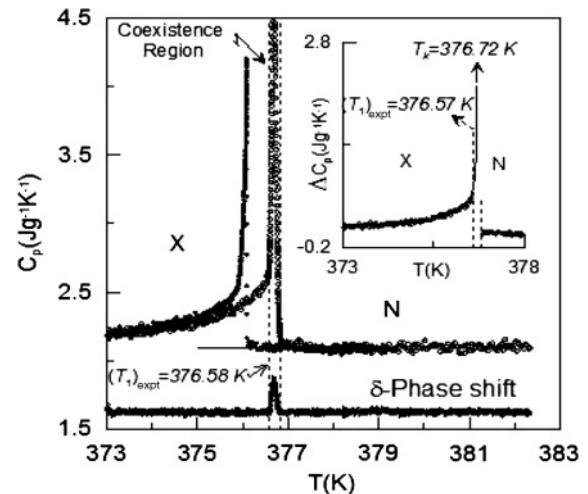


FIG. 5. Heat-capacity measurements for CB7CB in the region of the N_X -to- N phase transition. Cooling and heating runs are represented by full and empty symbols, respectively. The δ -phase shift (arb. units) accounts for the narrow coexistence region.

it can be assumed that two order parameters are involved in the transition, but the x-ray results deny the existence of a layer density wave, i.e., long-range translational order is absent. However, it is possible that coupling between the nematic-like orientational order and a tilt angle could provide a mechanism for a Landau tricritical transition. The problem is a definition for the tilt angle, which in smectic-*C* phases is defined with respect to the layer normal, but in the N_X phase there is no obvious axis against which to measure the tilt. If there were a helical structure, then it would be possible to define the tilt with respect to the helix axis.

The contrast between the variation of the heat capacity in the region of the N_X -*N* transition and the usual behavior measured in the vicinity of a nematic-isotropic transition is clearly seen by comparing Fig. 5 with measurements around the *N*-*I* transition (see the supplemental material [61]). The variation of heat capacity with temperature around the low-temperature nematic to the high-temperature nematic phase of CB7CB shows a highly asymmetric peak. This behavior is consistent with the mean-field Landau model in which the phase above the transition (the nematic phase in this case) exhibits a linear heat capacity (an α critical exponent of zero) that fully corresponds to the heat capacity background. This singular behavior has been observed to describe well the smectic-*C*-nematic phase transition in the vicinity of a tricritical point [24,25].

V. DIELECTRIC STUDIES AND THE EFFECT OF ELECTRIC FIELDS

Details of the technique used to measure the dielectric properties of aligned liquid crystals have been described in an earlier paper [10]. Cells that are 50 μm thick and have gold electrodes were used, which, for CB7CB, give a random planar alignment. The dielectric anisotropy of CB7CB at low frequencies is positive and so it enables the use of a dc bias voltage (35 V) to generate homeotropic alignment for the sample. This configuration allows the measurement of the parallel component of the electric permittivity. The process of alignment and realignment is completely reversible. The setup used in our work allows measurements to be performed over the range of frequencies from 10^2 to 1.8×10^9 Hz, although only the range 10^6 to 1.8×10^9 Hz is shown here in the figures.

Previous measurements have been reported by us [10,26] and others [27] on symmetric dimers containing two mesogenic groups joined by an alkyl chain connected to the terminal groups through an ether link. This linking group has an associated dipole moment, and so there is a component of the molecular dipole perpendicular to the dipolar axis of the terminal groups. In contrast, in CB7CB the dipole moment is located solely in the nitrile group attached to the terminal groups. Measurements of the static parallel (ϵ_{para}) and perpendicular (ϵ_{perp}) permittivities are shown in Fig. 6. These static permittivities of CB7CB vary with temperature in a manner similar to those measured for other symmetric dimers.

The transitions to the nematic and the low-temperature nematic phase, N_X , are clearly reflected by the dielectric measurements. The most notable feature of these results is for the mean or scalar permittivity, $\bar{\epsilon} = \frac{1}{3}(\epsilon_{\text{para}} + 2\epsilon_{\text{perp}})$, which differs increasingly from the extrapolated isotropic value,

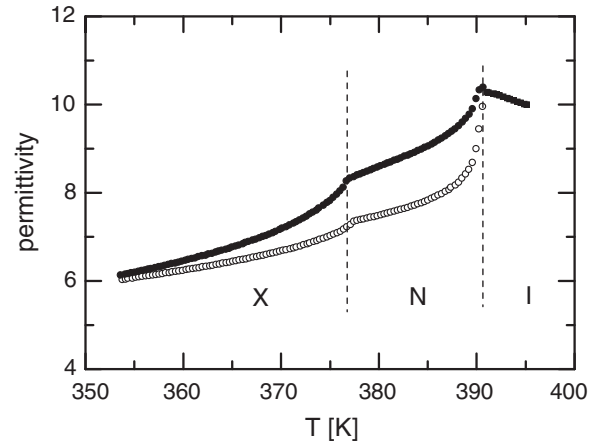


FIG. 6. The principal components of the permittivities, extrapolated to zero frequency, for CB7CB shown as a function of temperature: parallel ($\epsilon_{\text{para}} = \bullet$) and perpendicular ($\epsilon_{\text{perp}} = \circ$) components.

starting at the nematic-to-isotropic transition, with decreasing temperature through both the *N* phase and the following N_X phase. This indicates that the average molecular mean-square dipole moment is changing very significantly with temperature. Such a dramatic change is only possible through a substantial change in the average molecular structure. The terminal dipolar groups contribute to both components of the permittivity, though the relative contributions depend on the conformation of the molecule. Since CB7CB is a flexible molecule, the distribution of different conformations with varying net dipole moments is very strongly temperature-dependent in the liquid-crystalline phases. Such behavior is predicted by a generic model for the orientational and conformational order of liquid-crystal dimers, which also reveals a nematic-nematic transition for odd dimers [28,29]. At this transition, there is a discontinuous change in the conformational distribution showing a growth in the proportion of linear conformers with respect to bent on entering the low-temperature nematic phase.

Initially on cooling from the isotropic phase, the value of the parallel component of the permittivity shows a small increase, which is expected for low molecular weight mesogens having a positive dielectric anisotropy. However, for symmetric mesogenic dimers, including CB7CB, the parallel permittivity then decreases in the nematic phase with a further decrease in temperature. The variation of the perpendicular component of the permittivity in CB7CB is similar to that recorded for monomeric and dimeric mesogens having a positive dielectric anisotropy. The observed variation of the parallel and perpendicular permittivities of symmetric dimers can be modeled by changes in the conformational distribution caused by the increase of orientational order with a decrease in temperature (see Sec. VII). In the low-temperature N_X phase, which supercools strongly, the dielectric anisotropy [$\Delta\epsilon = (\epsilon_{\text{para}} - \epsilon_{\text{perp}})$] becomes close to zero, and may change sign from positive to negative at lower temperatures.

The real and imaginary parts of the parallel and perpendicular electric permittivities measured as a function of frequency for temperatures in the nematic and low-temperature nematic

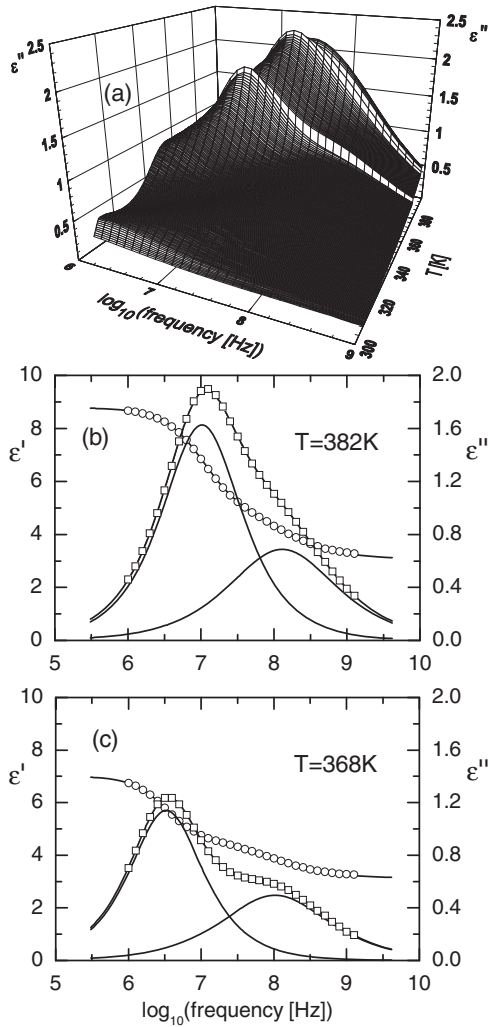


FIG. 7. The parallel component of the permittivity ($\epsilon' =$ real part and $\epsilon'' =$ imaginary part) of CB7CB. (a) Frequency and temperature dependence of ϵ'' . (b) Frequency dependence of ϵ' (○) and ϵ'' (◻) in the N phase. (c) Frequency dependence of ϵ' and ϵ'' in the N_X phase. In (b) and (c), the circles and open squares represent experimental points while the full lines are fits to the data using Eq. (3) and show the contributing modes. Parameters of the fit are given in Table I.

phase are given in Figs. 7 and 8. Dielectric absorption is measured by the imaginary part of the permittivity, while the real part of the permittivity measures the capacitance response. The dipolar moieties of CB7CB are associated with the terminal cyanobiphenyl groups in the molecule.

In a uniaxial phase, such a structure is expected to have two modes of dielectric relaxation associated with the rotational diffusion of the molecules. The low-frequency mode is due to an end-over-end or flip-flop motion of the dipolar groups parallel to the director. A high-frequency mode is associated with precessional motion of the dipolar groups about the director. These modes contribute to the dielectric absorption (imaginary part of the complex permittivity) of the parallel and perpendicular components to different extents, depending on the alignment of the director in the measurement cell. A three-dimensional representation of the variation of the imaginary part of the permittivity with frequency and temperature is

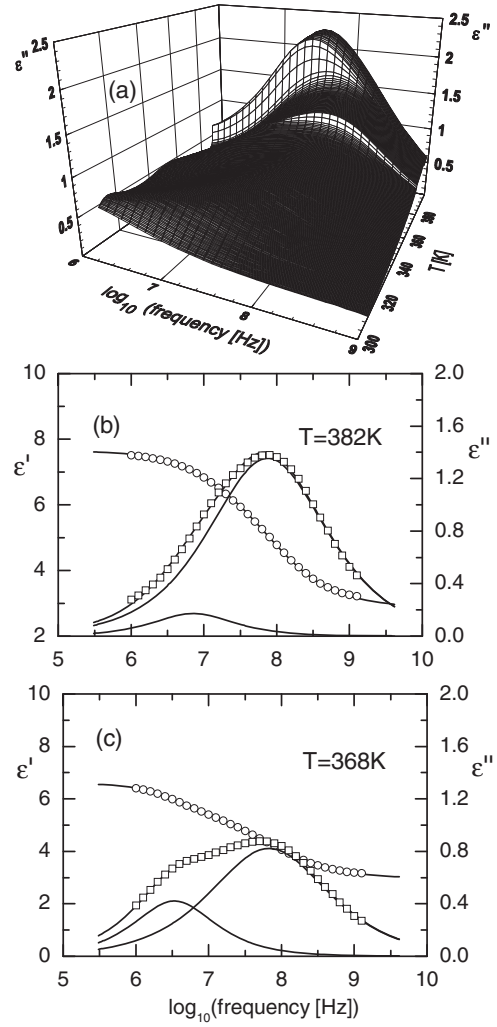


FIG. 8. The perpendicular component of the permittivity ($\epsilon' =$ real part and $\epsilon'' =$ imaginary part) of CB7CB. (a) Frequency and temperature dependence of ϵ'' . (b) Frequency dependence of ϵ' (○) and ϵ'' (◻) in the N phase. (c) Frequency dependence of ϵ' and ϵ'' in the N_X phase. In (b) and (c), the circles and open squares represent experimental points while the full lines are fits to the data using Eq. (3) and show the contributing modes. Parameters of the fit are given in Table I.

given for the two alignment directions of the liquid crystal in Figs. 7(a) and 8(a).

Experimental measurements of the frequency dependence of the permittivity have been analyzed using the Havriliak-Negami function,

$$\epsilon(\omega) - \epsilon_\infty + i \frac{\sigma_{dc}}{\epsilon_0} = \sum_{j=1,2} \frac{\delta \epsilon_j^0}{[1 + (i\omega\tau_j)^{\alpha_j}]^{\beta_j}}, \quad (3)$$

where $\delta \epsilon_{j=1,2}^0$ are the strengths of the two dielectric modes 1 and 2, ϵ_∞ is the extrapolated high-frequency permittivity, and σ_{dc} is the dc conductivity. The relaxation time, τ_j , is related to the frequency of maximum dielectric loss, and α_j and β_j are parameters that describe the shape of the relaxation spectra: $\alpha = \beta = 1$ corresponds to a simple Debye relaxation. The results of fitting the experimental measurements to Eq. (3) in the nematic phase at a temperature of 382 K and in the

TABLE I. Fitting parameters in Eq. (3) for the low-frequency (mode 1) and high-frequency (mode 2) contributions to the dielectric absorption as given in Figs. 7 and 8.

Phase temperature (K)	Alignment	α_1	α_2	β_1	β_2
Nematic phase N (382), Fig. 7(b)	parallel	0.92	0.75	1.0	1.0
Nematic phase N (382), Fig. 8(b)	perpendicular	0.91	0.70	1.0	1.0
Low-temperature nematic phase N_X (368), Fig. 7(c)	parallel	0.97	0.75	1.0	1.0
Low-temperature nematic phase N_X (368), Fig. 8(c)	perpendicular	0.91	0.70	1.0	1.0

low-temperature N_X phase at a temperature of 368 K for both parallel and perpendicular director alignments are given in Figs. 7(b) and 7(c) and Figs. 8(b) and 8(c), respectively, and the fitting parameters are given in Table I.

The dielectric relaxation results obtained in the nematic phase are as expected. For the homeotropic alignment (with bias), the parallel component of the permittivity is detected, and the low-frequency relaxation (flip-flop) predominates, with a contribution from the high-frequency precessional mode [see Fig. 7(b)]. Conversely, for the planar alignment of the liquid crystal, which samples the perpendicular component of the permittivity, the high-frequency mode predominates over the temperature range of the nematic phase, with a very small contribution from the low-frequency mode [see Fig. 8(b)].

At the transition from the nematic phase to the low-temperature N_X phase, the parallel component of the imaginary part of the permittivity shows contributions from both modes. As the temperature is reduced further, the amplitude of the low-frequency absorption decreases relative to the high-frequency mode [see Fig. 7(a)]. Measurements in the low-temperature phase of the perpendicular component of the dielectric absorption (planar alignment, no bias) are more remarkable [see Fig. 8(a)]. At the transition from the nematic phase there is a sudden appearance of the low-frequency relaxation mode, which persists to lower temperatures, although its amplitude decreases. This could mean that the planar alignment of the sample has become disordered. Applying a bias voltage to the low-temperature liquid-crystal phase now has no effect on the strength of the absorption, suggesting the effect is not a consequence of director misalignment at the transition. The simplest explanation is that the average axis of the longitudinal dipole moment has tilted, so that the low-frequency mode contributes to both the parallel and perpendicular components of the permittivity.

The dielectric anisotropy of CB7CB in the nematic phase is small but positive. In the N_X phase, the dielectric anisotropy

decreases rapidly with decreasing temperature, and may even reach zero. Thin films of planar aligned CB7CB can be switched from an optically transmitting state to a homeotropic black state, although large voltages up to 50 V across 5 μm are required. In the nematic phase, switching is reversed on removal of the applied voltage; however, it appears that in the N_X phase the switching is bistable. After switching in the N_X phase and removal of the voltage, the original texture is only recovered by heating to the nematic or isotropic phase and then cooling. Sample images from a switching sequence for the N_X phase are shown in Fig. 9. During switching, the N_X phase passes through a number of different optical states.

Dark lines develop in a direction perpendicular to the rubbing direction of the planar cell, and eventually spread over the whole sample to form the homeotropic switched state. This latter behavior is consistent with the small but positive dielectric anisotropy of CB7CB in the N_X phase.

VI. MAGNETIC RESONANCE STUDIES OF CB7CB

A. ESR spectroscopy

The ESR spectrum of the cholestane spin probe [30] was measured as a function of temperature in the isotropic, nematic, and the low-temperature nematic phase. The spectra are shown as a stack plot in Fig. 10 with high temperature at the front and low temperature at the back. In the isotropic phase, there are three well-resolved hyperfine lines, and these are preserved in the nematic phase but with a smaller spacing. This shows that the director is uniformly aligned parallel to the relatively weak magnetic field (~ 0.3 T) of the ECS 106 Bruker EPR spectrometer, consistent with the x-ray scattering investigation that used a higher magnetic field. On entering the low-temperature N_X phase, the spectrum changes significantly and two additional lines appear; the high-field components of these are apparent at the back of the stack plot in Fig. 10. Their appearance is consistent with the nonuniform alignment

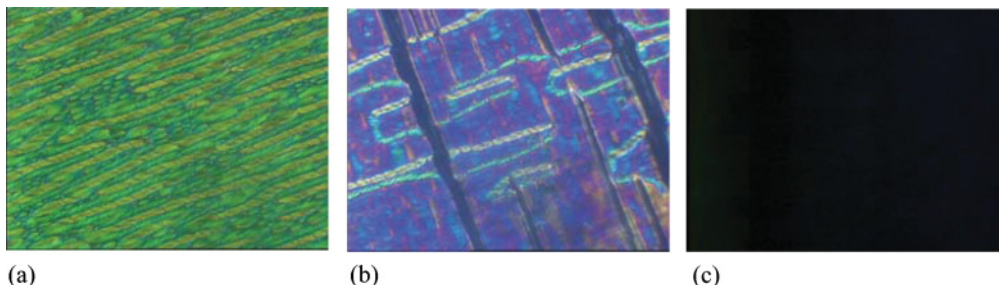


FIG. 9. (Color online) The effect of a voltage applied (10 Hz triangular) across a planar aligned sample (100°C) of the N_X phase of CB7CB on its optical texture. (a) Zero field, (b) field of 4 MV m^{-1} , and (c) after the electric field is removed from the fully switched state.

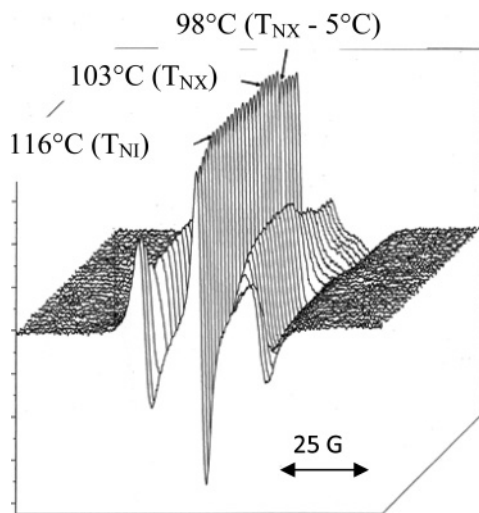


FIG. 10. A stack plot of the ESR spectra of a cholestane spin probe dissolved in CB7CB shown as a function of temperature. The vertical axis is a derivative of the spectral intensity in arbitrary units, while the horizontal axis is the scanned magnetic-field strength.

of the director with respect to the magnetic field; this confirms the results of our dielectric study described in the previous section. In fact, it was the nonuniform alignment of the director in the N_X phase that first suggested that the low-temperature phase had unusual properties and structure [18]. Rotation of the sample about an axis orthogonal to the field caused the spectrum to change, which indicates that the magnetic field (~ 0.3 T) is too weak to align the phase. After rotation through 90° , the spectrum shows, surprisingly, that the director is uniformly aligned with respect to the magnetic field. Rotation by a further 90° produces the original nonuniform alignment with respect to the field. It is difficult to understand the distribution of the director in this sample, especially as the x-ray experiments show that the director is uniformly distributed around the magnetic-field direction. However, a simple model for the director distribution consistent with these results would be for a phase in which the director adopts a helical distribution. When the helix axis is aligned parallel to the magnetic field, the director would be uniformly aligned to the field and the ESR spectrum would contain just three hyperfine lines, as observed. Then, when the sample is rotated by 90° about an axis orthogonal to the magnetic field, so that the helix axis is orthogonal to the field, the director would be randomly distributed in a plane containing the magnetic field. The ESR spectrum would now correspond to a two-dimensional powder pattern in which the dominant spectral features would correspond to the parallel and perpendicular components of the hyperfine tensor. We should note that the unusual results of the ESR experiments are also shown by the analogous odd dimer, CBO6CB, where the unusual behavior is even more pronounced [31].

B. Deuterium NMR spectroscopy

It has been claimed [32] that CB7CB forms a biaxial nematic, and given the bent form for molecules of this odd dimer, such a suggestion was not unreasonable. In order to test this identification, we have studied the deuterium NMR spectra

of CB7CB- d_4 using a Varian Infinity Plus 300 spectrometer and a quadrupolar echo sequence. The temperature was controlled to within $\pm 0.1^\circ\text{C}$ with a Varian temperature control unit whose scale was calibrated using the nematic-isotropic transition temperature for CB7CB of 116.5°C . In the present investigation, the specifically deuterated mesogen was distributed in the pores of a controlled porous glass (CPG3000B, obtained from Millipore, NJ). In this way, the director is aligned by the randomly distributed glass surface and not by the uniform high magnetic field (~ 7 T) of the NMR spectrometer. The resultant powder pattern for the high-temperature nematic phase, shown in Fig. 11(a), demonstrates that the director is randomly distributed in three dimensions.

The spectrum contains two dominant features: one is the outer shoulders corresponding to the parallel components of the quadrupolar splitting tensor, and the other is the inner horns, the positions of which are determined by the perpendicular component of the quadrupolar splitting tensor. The occurrence of just these two features shows that the phase is uniaxial in keeping with the earlier assignment [18]; for a biaxial phase, each of the horns would be split into two. The other check on the symmetry of the high-temperature phase is that the parallel splitting is twice that for the perpendicular component, at least to within the experimental error, which is determined by the spectral linewidth.

On forming the low-temperature N_X phase, the uniaxial powder pattern persisted, as may be seen from Fig. 11(b), but with slightly smaller splittings and sharper lines to those of the N phase. We see, therefore, that the low-temperature nematic phase is not biaxial, as had been supposed [32]. However, a second uniaxial powder pattern also appeared but with splittings larger than those of the first. The origin of the second uniaxial powder pattern with the larger quadrupolar splittings is a puzzle but might have been associated with the large surface area to which the N_X phase is exposed when creating thin films. To check this possibility, we were able to obtain a sample of the N_X phase with a partially random distribution of the director. This was achieved by heating the sample outside of the magnetic field of the spectrometer into the N phase and then cooling it until the N_X phase appeared. At this point, the sample was placed into the probe, which was held at 100°C . When the temperature had equilibrated, the NMR spectrum shown in Fig. 11(c) was measured. We note that the shoulders seen in Fig. 11(c) are now more intense and sharper than those in Fig. 11(b), indicating that the director is partially aligned by the magnetic field, but that there are still two powder patterns. This clearly demonstrates that the observation of two spectra observed when the N_X phase is dispersed in the CPG does not result from the containment in small pores.

Deuterium NMR spectra were also measured for the aligned N and N_X phases in the bulk, and these enabled accurate values to be determined for the orientational order parameter for the C-D bonds in the equivalent $1''$ and $7''$ positions of the heptyl chain and hence that for the para-axis of the mesogenic groups to be estimated.

A selection of the deuterium spectra is shown in Fig. 12 for CB7CB- d_4 ; in both nematic phases, the good uniformity of the director alignment is indicated by the sharpness and symmetry of the spectral lines. At 115°C in the

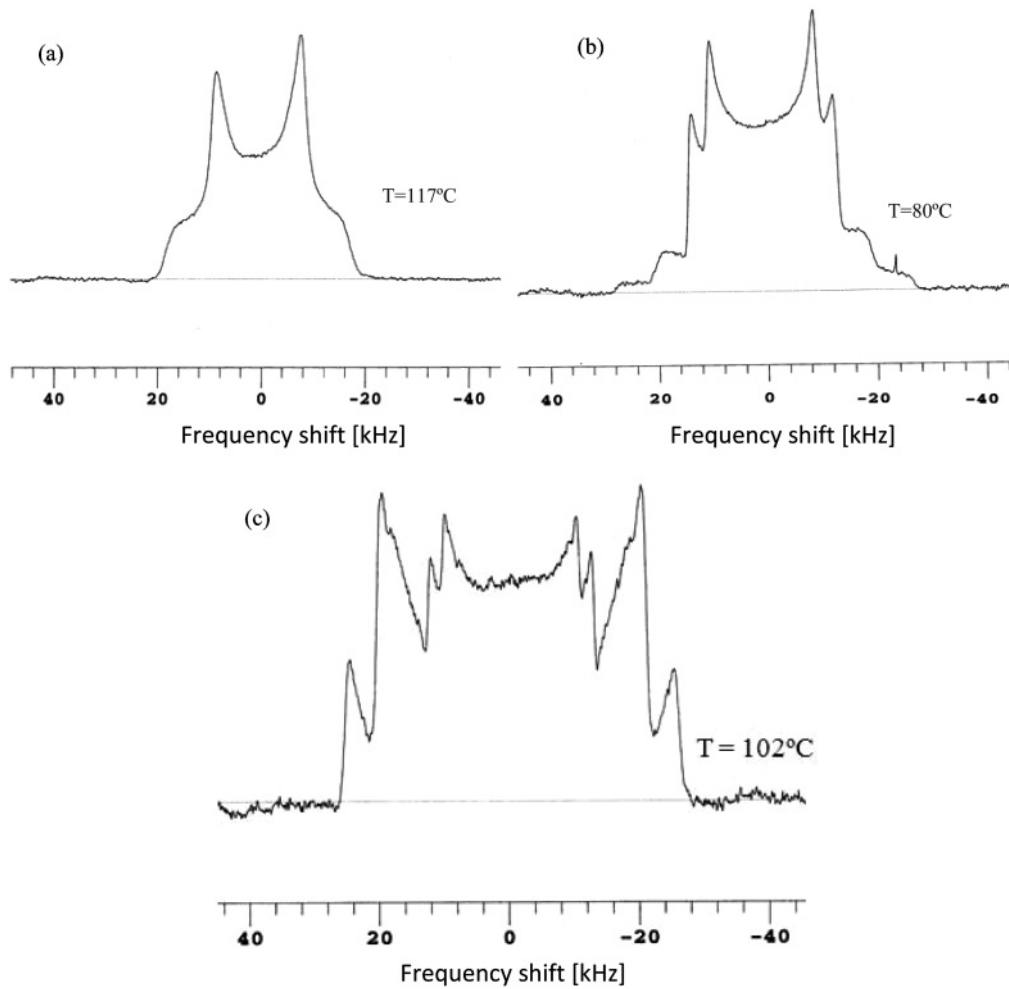


FIG. 11. The deuterium NMR spectra of CB7CB- d_4 (a) in the N phase at 117 °C randomly distributed in the CPG, (b) in the supercooled N_X phase at 80 °C randomly distributed in the CPG, and (c) in the partially random distribution for the bulk sample of the N_X phase at 102 °C. The vertical axis is the spectral intensity in arbitrary units, while the horizontal axis is a scale of frequency shifts relative to the center of the spectra.

high-temperature nematic phase, the spectrum consists of an intense quadrupolar doublet originating from the 1'' and 7'' deuterons. In addition, there is another quadrupolar doublet with a slightly smaller splitting and a much weaker intensity. Chemical shift measurements in a low-order nematic host suggest that this weak doublet originates from aromatic deuterons. On lowering the temperature to 106 °C, there is the expected increase in both quadrupolar splittings. However, in addition there is now another weaker quadrupolar doublet with a larger splitting than the other two. It is likely that the new quadrupolar doublet is associated with the N_X phase. This association is confirmed by the significant increase in its intensity at the transition of 103 °C. In the supercooled N_X phase at 96 °C, the two dominant quadrupolar splittings are still apparent. At 96 °C, we see that one of the quadrupolar splittings has increased, whereas that of the other quadrupolar doublet has decreased with respect to the splitting seen in the N phase. It is of particular importance, as we shall see, to note that whereas the intense quadrupolar doublet is split into two strong doublets on entering the N_X phase, the weaker quadrupolar doublet does not appear to be so split. Of course,

the second weak doublet might be obscured under one of the strong quadrupolar doublets. However, this explanation would be inconsistent with the increase in the intensity of the weak doublet with respect to one of the strong quadrupolar doublets; indeed, as expected, this relative intensity grows by about a factor of 2. We conclude, therefore, that the weak quadrupolar doublet from the aromatic deuterons does not split into two doublets on entering the N_X phase, unlike the strong doublet from the 1'' and 7'' methylene deuterons.

The mesogen CB7CB is readily supercooled in the bulk, and so it was possible to measure the quadrupolar splittings for the 1'' and 7'' deuterons in the low-temperature nematic phase over a wide range of temperatures as well as in the high-temperature nematic phase. The results for these measurements are shown in Fig. 13

The single quadrupolar splitting jumps from zero at the N - I transition in keeping with its first-order character. The splitting then increases relatively rapidly in the N phase, growing by almost 70% before the transition to the N_X phase occurs. At this transition, a second larger quadrupolar doublet appears having increased discontinuously from the value in

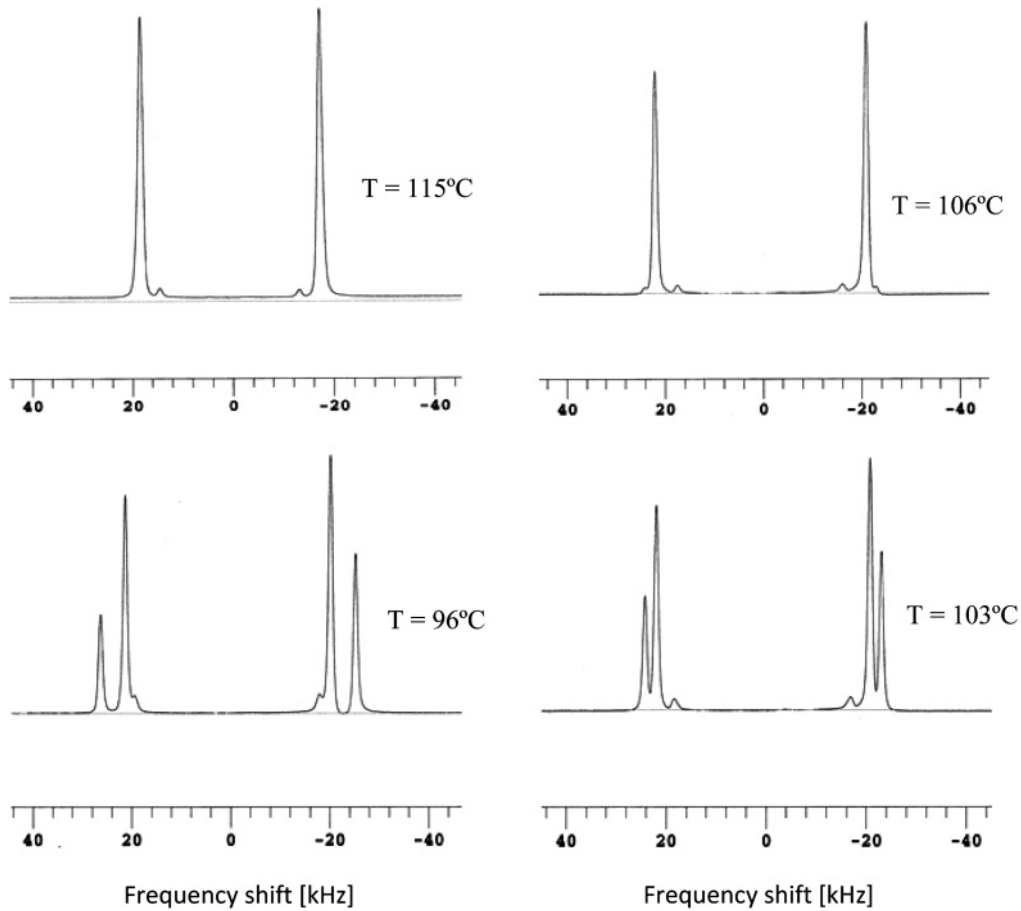


FIG. 12. The deuterium NMR spectra of CB7CB- d_4 aligned by a magnetic field of 7.05 T. From top, clockwise: nematic phase (115 °C), nematic phase (106 °C), N_X phase (103 °C), and N_X phase (96 °C). The vertical axis is the spectral intensity in arbitrary units, while the horizontal axis is a scale of frequency shifts relative to the center of the spectra.

the preceding N phase. Again, this is in keeping with the first-order character of the N_X - N transition. In contrast, the other quadrupolar splitting in the N_X phase appears to have changed continuously from that in the N phase. In view of the first-order character of the N_X - N transition, this suggests that there are two competing factors, one increasing the quadrupolar splitting and the other decreasing it. Within the N_X phase, the factor causing the smaller splitting to decrease is dominant. Over the extensive range of the supercooled nematic phase, the rate of increase of the larger splitting seems to be comparable to the rate of decrease for the smaller splitting. As a consequence, the average of the two splittings, also shown in Fig. 13, is seen to vary only slightly with temperature. The quadrupolar splitting for the doublet having a weak intensity is also shown in the figure. In the N phase, its variation parallels that for the $1''$ and $7''$ deuterons, increasing with decreasing temperature. However, at the N_X - N transition, it increases slightly, but unlike the $1''$ and $7''$ deuterons, the peaks are not split; instead, the single quadrupolar splitting parallels the mean of the two splittings for the $1''$ and $7''$ deuterons in the N_X phase.

The appearance of two quadrupolar splittings for the $1''$ and $7''$ deuterons in the N_X but not the N phase is an especially striking and, presumably, definitive feature of this new nematic phase. We need, therefore, to understand the origin of these

and their opposing temperature dependences. In fact, there are a variety of explanations, and we shall consider the most

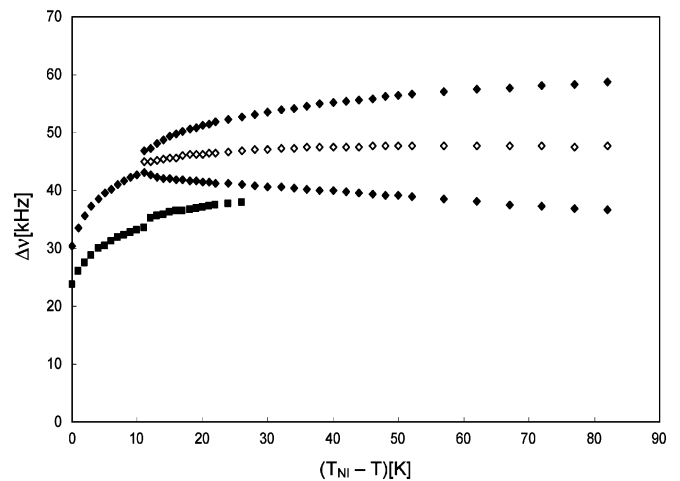


FIG. 13. The dependence of the quadrupolar splittings, $\Delta\nu$, on the shifted temperature $(T_{NI} - T)$ for the $1''$, $7''$ deuterons (\blacklozenge) and for the low-intensity doublet (\blacksquare) in the N and N_X phases. The average of the two splittings for the $1''$ and $7''$ deuterons in the N_X phase is shown as (\diamond).

likely of these and the extent to which they are consistent with other observations in our investigation before opting for one of them.

1. Loss of equivalence of the 1'' and 7'' deuterons

The sample, CB7CB- d_4 , contains two deuterons in the 1'' position of the heptyl chain and two more in the 7'' position corresponding to the first and last methylene groups adjacent to the mesogenic groups. These two positions are structurally equivalent, and this equivalence is apparent from the NMR spectrum in the N phase (see Fig. 12). In the N_X phase, this equivalence could be lost depending on the phase structure. We have excluded this possibility by studying the monomer spin probe 8CB- d_2 , in which the 1'' methylene group is deuterated and dissolved in CB7CB. Since there is only one deuterated methylene group, the quadrupolar splitting should not split in the N_X phase. In fact, we do observe a significant splitting in the quadrupolar splitting for 8CB- d_2 on entering the N_X phase.

2. Nonuniform director distribution

This explanation is related to the development of nonuniformity in the director orientation. When the director distribution in a uniaxial liquid-crystal phase is uniform with respect to the magnetic field, then the deuterium NMR spectrum contains a single quadrupolar doublet for a set of equivalent deuterons. An example of a single quadrupolar doublet measured when the director of a uniaxial nematic is aligned parallel to the magnetic field is shown in Fig. 12. If now the director were to be rotated so that the director remains uniform but aligned at an angle φ to the field, then a single quadrupolar doublet would still be observed, but now the splitting is reduced from $\Delta\nu_0$, when the director is parallel to the field, to $\Delta\nu_0 P_2(\cos\varphi)$. Here the angular dependence is contained in the second Legendre polynomial, $P_2(\cos\varphi)$. If the director adopted just two orientations with respect to the field, and the exchange between these is slow on the NMR time scale of 10^{-4} s, then two quadrupolar doublets would be observed. Now not only would the splittings be different, but their intensities would also vary depending on the director orientational distribution function, $p(\varphi)$. The relative sharpness of the spectral lines in the N_X phase would require that the director distribution function is peaked at just two values of φ with different probabilities. The ratio of the quadrupolar splittings for various groups of equivalent deuterons will depend on the director orientations via the ratio $P_2(\cos\varphi_1)/P_2(\cos\varphi_2)$. The site-dependent factor $\Delta\nu_0$ has canceled, and so the ratio of splittings should be the same for all groups of deuterons in the molecule. As we have seen, this is not the case, for the splittings for the aromatic deuterons are the same, giving a ratio of unity whereas the ratio for the 1'' and 7'' deuterons varies from 1.14 at the N_X - N transition to 1.56 at about 70 °C below it. The explanation of the splitting of the intense quadrupolar splitting into two in the N_X phase based on a nonuniform director distribution may, therefore, be excluded.

3. Slow exchange between conformers

The doubling of the quadrupolar splittings in the N_X phase of an analog of CB7CB- d_4 has been explained by

Kumar *et al.* [33] in terms of the so-called generic model for liquid-crystal dimers [28,29]. In this, the dimers are taken to exist in just two conformers, one bent and the other a hairpin or linear, each with a different orientational order. In the nematic phase there is rapid exchange on the NMR time scale between the two conformers, so that the deuterium spectrum contains just a single quadrupolar doublet, as observed. However, at the transition to the N_X phase, it is assumed that the rate of conformational exchange is reduced and becomes slow on the NMR time scale [33]. It is to be expected that for CB7CB- d_4 , the larger quadrupolar splitting would originate from the hairpin conformer and the smaller from the bent. The relative intensity of the two doublets would be determined by the conformational distribution function. Theory predicts that below the nematic-nematic transition, the hairpin conformer will have the larger relative probability, and that as the temperature is reduced, its probability will grow [28,29]. This generic prediction is in marked contrast to the behavior observed for CB7CB- d_4 . In addition, since the orientational order of the N_X phase will grow with decreasing temperature, it is expected that the order of both conformers will also grow [28,29]. Again this predicted behavior is in marked contrast with experiment where the splitting of the conformer(s) with the smaller order decreases and that for the more ordered conformer(s) increases (see Figs. 12 and 13). Thus this proposed explanation seems to be in conflict with what is observed. We shall return to the validity of the proposal by Kumar *et al.* [33] in Sec. VII A when we show a more realistic prediction of the conformational distribution.

4. Chirality and loss of equivalence of the deuterons in the methylene groups

We have seen in Sec. B1 that the different quadrupolar splittings in the N_X phase could not be explained by the inequivalence of the 1'' and 7'' deuterons. This leads us to consider the possibility that the splitting of the quadrupolar doublet in the NMR spectrum in the N_X phase results from the inequivalence of the two deuterons in a single methylene group. This could result if the two C-D bonds made different angles with the principal axes of the Saupe ordering matrix. This would certainly be the case in many of the conformers for the CB7CB dimer. However, dynamic exchange between conformers leads to a change in the effective or average structure and hence symmetry. For a frame set in, say, the 1'' methylene group, this average structure will possess just C_s point-group symmetry; that is the identity and, more importantly, a mirror plane that bisects the DCD bond angle. It is this effective plane of symmetry that results in the equivalence of the two deuterons on the methylene carbon; they are described as enantiotopic.

A simpler molecule with the same characteristics is ethanol- d_2 where the deuterons are in the methylene group. These are also enantiotopic because the rotation of the methyl and hydroxyl groups about the bonds to the methylene carbon means that the effective symmetry is again C_s . In an achiral nematic host, the two deuterons are equivalent and a single quadrupolar doublet will be observed in the deuterium NMR spectrum, provided the dipolar interaction is small. However, it is observed that when ethanol- d_2 is dissolved in a chiral

solvent, such as poly- γ -benzyl-L-glutamate (PBLG) dissolved in chloroform, there are two quadrupolar doublets [34,35]. This inequivalence of the two deuterons is attributed to the loss of the plane of symmetry caused by the chirality of the nematic host; it reflects the fact that the ordering of the solute is determined by the symmetry of both the solvent and the solute.

It seems likely, therefore, that for CB7CB- d_4 , another explanation for the splitting of the quadrupolar doublet for the 1'' and 7'' deuterons is that the N_X phase is chiral, or has chiral domains of opposite handedness. The same symmetry argument does not apply to the quadrupolar doublet with the small intensity that we have assigned to aromatic deuterons. Indeed, we would not expect this to be split into two in the N_X phase simply because given the low extent of deuteration, only one such deuteron would be contained in each molecule.

There is another piece of evidence that is also consistent with this explanation of the splitting of the 1''- and 7''-quadrupolar doublets in the N_X phase of CB7CB. In the first NMR investigation of CB7CB, its orientational order was explored using a deuterated spin probe [18]. This was perdeuterated anthracene- d_{10} , which has D_{2h} point-group symmetry so that the four α -deuterons are strictly equivalent, as are the four β -deuterons and the two γ -deuterons. However, the difference in the quadrupolar splittings for the α and γ deuterons for anthracene- d_{10} is small, although it has been resolved when it is dissolved in some nematogens [36], but not in CB7CB. Accordingly, only two quadrupolar splittings were observed, and these were not split further in the N_X phase, which at the time was not surprising since it was thought to be a smectic- A phase. The fact that there were no further splittings is inconsistent with the possible explanation given in Sec. B 2. However, it is certainly consistent with the explanation considered here. Since anthracene has D_{2h} point-group symmetry, the equivalence of the deuterons within the three sets results from three twofold rotation axes, and so the chirality of the nematic environment cannot remove this equivalence, as found in [18].

There is, however, one major difficulty with this explanation, and, as for the second of the other potential explanations, it is associated with the unequal intensities of the quadrupolar doublets in the N_X phase. If these two doublets result from the loss of the equivalence of the deuterons, then their intensities will be determined by the deuterons in the methylene groups. Since the extent of deuteration of CB7CB- d_4 is high, it is to be expected that each of the 1''- and 7''-methylene carbons will have two deuterons. Consequently, when they lose their equivalence in the N_X phase, the resulting quadrupolar

doublets should have the same intensities. At present, we cannot explain why the doublets in the experimental spectra have unequal intensities. Another point of interest is the ratio of the quadrupolar splittings for these doublets; this ranges from 1.11 at the N_X - N phase transition to 1.57 some 60 °C below it. The ratio at low temperatures is certainly very large, especially in comparison with that found in studies of systems in which the chirality of the nematic solvent is not in doubt. Thus for 5CB- d_{19} dissolved in PBLG/CHCl₃, the ratio for the splittings of the 1'' deuterons in the pentyl chain is only 1.04 [37]; however, the orientational order of the C-D bonds in this chiral nematic is about 20 times smaller than that in the N_X phase of CB7CB at its highest temperature. As we have seen, the ratio of splittings does increase significantly with decreasing temperature within the N_X phase, but similar measurements of the temperature dependence do not seem to be available for the PBLG systems.

5. Orientational order

In addition to aiding the determination of the structure for the low-temperature nematic phase, deuterium NMR spectroscopy can also be used to provide a measure of the orientational order of both nematic phases. The element, S_{zz} , of the Saupe ordering matrix for the para-axis of the cyanobiphenyl mesogenic groups is related to the quadrupolar splittings $\Delta\nu$ for the deuterons by

$$S_{zz} = (2/3)\Delta\nu/q_{CD}P_2(\cos\theta). \quad (4)$$

Here, $P_2(\cos\theta)$ is the second Legendre polynomial, θ is the angle between the C-D bond and the z axis, and q_{CD} is the quadrupolar coupling constant for a deuteron attached to an aliphatic carbon. We shall take q_{CD} to be 168 kHz and θ as the tetrahedral angle. In the N_X phase, there are two quadrupolar splittings, but as we have seen in the previous section, if their origin is the chirality of the phase, then the average of the two is expected to give the order parameter for the achiral N_X phase. A selection of the measured values of the quadrupolar splittings is given in Table II for both nematic phases as a function of the shifted temperature, $T_{NI}-T$. We see that at the nematic-isotropic transition, the order parameter for the mesogenic groups is 0.305, which compares favorably with that found for the corresponding ether-linked dimers [38]. There is a small increase in the order parameter at the N_X - N transition, and this increases slightly on lowering the temperature in a manner consistent with the order parameters found in the nematic phase. As we shall see in the next section, these results facilitate the comparison of theoretical predictions with experiment.

TABLE II. The order parameter S_{zz} calculated from the major quadrupolar splitting in the N phase and from that characteristic of the achiral N_X phase.

$(T_{NI}-T)/K$	Nematic phase, N			Low-temperature achiral nematic phase, N_X					
	0	8	14	15	22	31	41	55	75
$\Delta\nu$ /kHz	25.6	39.1	43.1	45.0 ^a	46.3 ^a	47.1 ^a	47.6 ^a	47.8 ^a	47.6 ^a
S_{zz}	0.305	0.465	0.513	0.531 ^b	0.551 ^b	0.561 ^b	0.567 ^b	0.569 ^b	0.567 ^b

^aThe mean of the two quadrupolar splittings in the N_X phase.

^bCalculated from the mean of the quadrupolar splittings in the N_X phase.

VII. QUANTUM- AND STATISTICAL-MECHANICAL CALCULATIONS

A meaningful theoretical model for a flexible dimer must take into account the structure of the mesogenic groups and the flexibility of the connecting chain. The present work uses the surface interaction (SI) model [39] to describe the orientational ordering of the dimer. This is a generalization of the Maier-Saupe theory, which takes into account molecular shape. It results in a phenomenological potential of mean torque equivalent to that for biaxial molecules [40] but with the parameters clearly related to the molecular structure. The parametrization is defined such that the surface normal prefers to be perpendicular to the director, and so the molecular long axis tends to align parallel to the director axis.

The molecular flexibility in the dimer CB7CB is accounted for by using two models, and results are reported for both. The traditional, and usually adequate, approach to modeling the effects of alkyl chains is to use the rotational isomeric state (RIS) approximation [41]. This recognizes that for groups attached to a carbon-carbon single bond, there are three minima in the torsional potential as a function of the dihedral angle: the lowest is labeled as *trans*, and the others as *gauche*⁺ and *gauche*⁻. The RIS model only includes chain conformations corresponding to these energy minima for each carbon segment. In addition, the torsional potential for rotation about the C_{ar}-C_{al} bond is included with the energy minimum being when the C_{1'}-C_{2'} bond is orthogonal to the phenyl ring. In the calculations, those conformations with overlapping atoms are rejected because of steric overlap. Another model for the conformational states is to retain a continuous torsional potential (CTP) for rotation about each carbon-carbon single bond, and then use umbrella Monte Carlo sampling methodology [42] to obtain a representative distribution of chain conformations; again, conformers with overlapping atoms are rejected. The CTP model was also used here, and for some properties the results are in significantly better agreement with experiment than those using the RIS model.

The initial step in these simulations is the determination of the molecular geometry and the torsional potentials. These were obtained by geometry optimization at the DFT/B3LYP level with the 6-31g** basis set [43]. The torsional energies were then fitted to analytic expressions. To facilitate the calculations for molecules such as liquid-crystal dimers, geometry and energy calculations were performed for molecular fragments, for example ethyl- and butyl-benzene as well as 4-ethyl-4'-cyanobiphenyl [44].

A. Conformational distribution

Calculation of the conformational distribution for a flexible molecule gives an idea of the range of shapes that such a molecule may adopt. The SI model shows how the molecular shapes may adjust to the orienting potential in a nematic liquid crystal. This will tend to favor the more elongated conformers. In an idealized alkyl chain, all angles are equal to the tetrahedral angle. If only *trans*, *gauche*⁺, and *gauche*⁻ conformations are allowed, then two terminal groups connected by an odd number of carbon atoms of five or more can only make angles of 0° or 109° with each other. In a nematic

liquid crystal, the relative energies, and hence probabilities, of these two molecular structures would be determined also by the potential of mean torque. In the calculations for CB7CB reported here, the bond angles at the carbon atoms were calculated to be C_{ar}C_{ar}C_{al} = 121.6° and C_{al}C_{al}C_{al} = 113°, i.e., some 4° larger than the tetrahedral angle of 109°. These and other calculations were performed as a function of the orientational order parameter, S_{zz}, for the para-axis of the cyanobiphenyl mesogenic group.

The results of our calculations of the probability distribution for the angle β between the *para*-axes of the terminal cyanobiphenyl groups in CB7CB are given in Fig. 14 for S_{zz} equal to 0.30, which is the order parameter measured at the nematic-isotropic transition, and 0.46, which is that at about 8 K below the transition. For the RIS model, the distribution function has two narrow peaks around 15° and 119°, corresponding, respectively, to hairpin and extended V molecular shapes. Higher values of the order parameter promote the stability of the hairpin shape at the expense of the extended shape. Calculations using the continuous torsional potentials, shown in Fig. 14, for the angles between the terminal mesogenic groups result in much broader distributions for the angle with two maxima: one weak corresponding to about 30°, while the other stronger is at 120°. At first glance, the RIS and CTP distributions are qualitatively similar, however it is significant that for the CTP model, at higher values of the order parameter the more extended molecular shapes within the broad peak centered at 120° are stabilized at the expense of the less extended conformers. The associated changes for the hairpin conformers are seen to be much weaker.

Having calculated the conformational distribution function, various equilibrium properties for flexible molecules can be calculated. Such calculations have been made for the elastic constants, electric permittivities, and flexoelectric coefficients [44–46], and they show that some calculated properties of flexible dimers, viz., the bend elastic constant and the electric permittivity, are particularly sensitive to the details of the conformational distribution. To explore this further, the atomistic model has been extended to calculate the elastic constants for particular conformations of a simple mesogen, namely 4-*n*-pentyl-4'-cyanobiphenyl [46]. The results show that the calculated values for elastic constants depend strongly on the conformational state and hence the shape of the mesogenic molecules. This dependence is particularly marked for the bend elastic constant, K₃, which for certain bent conformations is predicted to be negative.

B. Electric permittivity

The absolute electric permittivity is a difficult quantity to calculate for condensed phases, and especially so for liquid crystals. However, neglecting effects of dipole correlations as well as anisotropic reaction and depolarizing internal fields, a simplified expression for the electric permittivity components of a uniaxial nematic liquid crystal can be written as [11]

$$\varepsilon_i = 1 + \frac{\rho}{k_B T} \langle \mu_i^2 \rangle. \quad (5)$$

Here *i* = para or perp, and ⟨μ_{*i*}²⟩ is the mean-square dipole along and perpendicular to the director. The variation of the

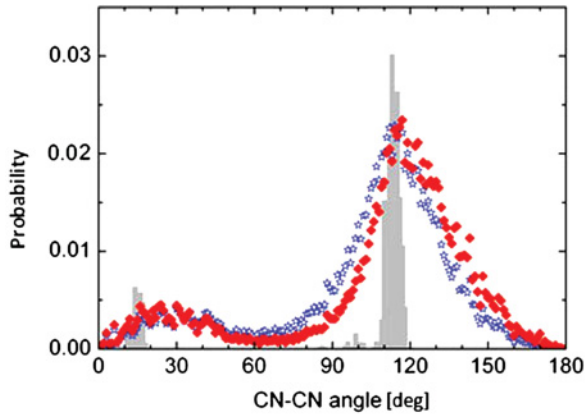


FIG. 14. (Color online) The probability distributions for the angle between the terminal mesogenic groups of CB7CB, calculated for the uniaxial nematic phase at two different values of the order parameter S_{zz} . Results for the continuous torsional potential are given for $S_{zz} = 0.30$ (open stars) and $S_{zz} = 0.46$ (filled diamonds). For comparison, the distribution obtained for the RIS model is shown as a histogram.

individual permittivity components with temperature in the nematic phase can be expressed in terms of the reduced variable:

$$\frac{\varepsilon_i - \varepsilon_{\text{iso}}}{\varepsilon_{\text{iso}} - 1} = \frac{\langle \mu_i^2 \rangle - \langle \mu_{\text{iso}}^2 \rangle}{\langle \mu_{\text{iso}}^2 \rangle}, \quad (6)$$

where the subscript “iso” indicates the isotropic phase.

Results for the reduced mean-square dipole components are shown in Fig. 15 for CB7CB. These were obtained with the SI model for the orientational potential using the RIS model and the continuous torsional potential model for the conformational energy. It is clear that there is a substantial difference between the predictions of the RIS and CTP models, and the latter is much closer to the experimentally observed temperature variation of the parallel and perpendicular components of the permittivity. The difference in behavior is easily understood from the probability distributions shown in Fig. 14. In the RIS model, decreasing the temperature increases slightly

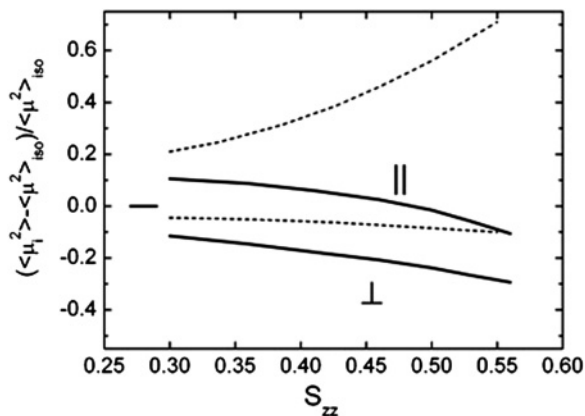


FIG. 15. Results for the parallel and perpendicular mean-square dipole moments of CB7CB calculated as a function of the order parameter, S_{zz} . Solid lines show the results obtained by MC sampling of conformations generated with CTP, while the dashed lines are those obtained by MC sampling of RIS conformers.

the small concentration of hairpin conformers. However, there is a large dipole moment associated with the hairpin dimer, and this is reflected in the significant increase of the parallel permittivity component with decreasing temperature in the nematic phase. In contrast, the calculated perpendicular component of the mean-square dipole only decreases slowly with temperature. While the RIS model fails to predict the experimental behavior, the CTP model predictions are more successful. Thus the parallel mean-square dipole moment shows an initial increase on cooling into the nematic phase followed by a steady decrease as the temperature falls further; see Fig. 6. This decrease is explained by the CTP conformational probability distribution. As the orientational order increases, so too does the amount of the more extended conformers. As their dipole moments decrease, the parallel component will also be reduced. It is also observed that the perpendicular component of the permittivity decreases with a decrease in temperature, and this can also be explained from the calculated CTP-based angle distribution. As the temperature falls, the order parameter increases, and the proportion of extended dimers also increases. Furthermore, because of the softness of the potential describing the alkyl chain conformations, the angle between the terminal dipolar groups increases slightly and the molecule becomes, on average, more linear. The effect of this is to reduce further the perpendicular mean-square dipole, and so the corresponding permittivity component also decreases with temperature.

This comparison of modeling and experimental results for the dielectric properties provides an important perspective on the behavior of molecules in nematic CB7CB. As the temperature falls, the molecules change their overall effective shape to become more extended, thereby increasing further the orientational order of the mesogenic terminal groups, as measured by NMR (see Table I). However, the calculations do not directly reveal anything of the structure of the low-temperature nematic phase. They do, however, suggest that the N_X phase is unlikely to be that predicted by the simple model of liquid-crystal dimers [28,29,33]. Thus for the more realistic model described here, the calculations of the mean-square dipole moment (see Fig. 15) and the elastic constants (see Fig. 17) do not reveal the nematic-nematic transition predicted by the simple model. Since the calculations were performed for the same range of order parameter as that found experimentally for both the N and N_X phase, it would seem that the absence of a nematic-nematic transition in the theoretical predictions does not support the identification of the low-temperature nematic phase as one with an enhanced concentration of hairpin conformers.

VIII. DISCUSSION

The objective of this major study of the liquid-crystal phases formed by CB7CB has been to determine the nature of the low-temperature liquid-crystal phase which appears on cooling from the nematic phase at 103 °C. The observed optical textures are reminiscent of tilted phases; in addition, they also suggest the formation of chiral domains of opposite handedness within the low-temperature nematic liquid crystal. In addition, x-ray examination of the material showed conclusively that there is no long-range layered structure

present, indicating that this new phase is also a nematic. The diffraction angles of the diffuse scattering peaks indicate that the phase is intercalated.

Calorimetry has characterized the transition between the nematic phase and the initially unknown nematic phase as weakly first-order, however the variation of heat capacity in proximity to the transition fits the Landau theory for the behavior close (within $\pm 0.1^\circ$) to a tricritical point. The existence of a tricritical point results from the coupling between two order parameters, which our measurements on CB7CB suggest are related to uniaxial orientational order and a tilt angle.

The dielectric anisotropy of CB7CB shows a discontinuity at the isotropic-to-nematic transition on cooling, and then continues to decrease through the nematic phase into the tentatively identified low-temperature nematic mesophase. This striking behavior in the nematic phase is explained, as we have seen, by a change in the conformational distribution with temperature and hence orientational order. Dielectric measurements on a mixture of a mesogen having a strongly positive dielectric anisotropy with a small concentration of rigid bent-core molecules have been reported [47]. These mixtures also show a marked reduction in the dielectric anisotropy with decreasing temperature, which is attributed to the influence of the bent-core molecule on the orientational distribution of the mesogen. The reduction in the dielectric anisotropy is paralleled by a strong reduction in the bend elastic constant, which the authors attribute to the development of a bend distortion of the director in the nematic phase that couples to the bent shape of the molecule.

Our measurements of the dielectric relaxation of CB7CB are consistent with the apparent development of a tilt in the low-temperature phase, since the low-frequency relaxation, characteristic of the parallel component of the permittivity, contributes to the perpendicular component in the low-temperature mesophase.

The ESR observations of a spin probe dissolved in CB7CB show that the nematic phase director becomes disordered in some manner at the transition to the low-temperature phase, which is consistent with the development of a uniform tilt in the structure.

The spectra obtained from deuterium NMR spectroscopy on CB7CB- d_4 are excellent and important. In a randomly aligned sample, they showed that both nematic phases were uniaxial. This is significant because the effective molecular shape of this dimer is highly biaxial and so might have formed a biaxial nematic [48], as had been suggested [32]. In the aligned nematic state, the spectra in the low-temperature phase show two pairs of well-resolved lines together with a much weaker single quadrupolar doublet. These persist over a considerable range of temperature as the low-temperature nematic liquid crystal supercools far below the freezing point of the compound. We consider a range of possible explanations that could account for the splitting of the quadrupolar doublet from the methylene deuterons that occurs on entering the N_X phase. The most reasonable of these appears to us to be the loss of equivalence of the two deuterium atoms attached to the carbon. This is known to occur if the phase is chiral [34,35]. The possible chirality of what should be an achiral phase is supported by microscopic observations of the ropelike

texture of the N_X phase when aligned in a uniform planar cell.

Calculations of the conformational distribution in CB7CB have been carried out using the surface interaction model with both the RIS model and continuous torsional potential for bonds in the connecting alkyl chain. The results using the continuous potentials provide good agreement between theory and experiment for the dielectric properties. In contrast, the RIS model fails completely to predict the temperature variation of the dielectric anisotropy found for CB7CB. These and other calculations have shown that for flexible dimers with odd numbers of methylene spacers, certain properties, specifically the bend elasticity and the dielectric properties, are very sensitive to the conformational distribution. Intriguingly, the calculated bend elastic constants can be negative for certain conformations of the dimer, which would promote spontaneous bending of the director, and the formation of a nematic phase in which the ground state for the orientation of the director is a permanent bend. This would be the bend equivalent of the twisted chiral nematic (cholesteric) phase.

In addition to the biaxial nematic phase, there have been a number of reports in the literature of possible nematic-nematic phase transitions [14,47,49–56]. The thermodynamic nature of these phase transitions depends on the symmetry of the adjacent phases. If the symmetries of the nematic phases are identical, then the transition will be first order, but transitions between nematic phases of different symmetries, such as that between a uniaxial nematic and a biaxial nematic, may be of first or second order, or tricritical. For the most part, the defining structural features of reported novel nematic phases remain unidentified. A uniaxial nematic-nematic phase transition has been predicted for main chain polymer liquid crystals [50], and experimentally observed in flexible copolymers of polyesters and polyesters having flexible spacers with odd numbers of methylene groups [51,52]. A first-order nematic-nematic transition has also been predicted [28,29] for a mixture of linear and bent conformers in odd liquid-crystal dimers resulting from a change in the proportion of linear and bent conformers together with their orientational order.

The unknown nematic N_X phase of CB7CB described in this paper is macroscopically uniaxial. Yet dielectric, ESR, and deuterium NMR suggest that at the transition from the high-temperature nematic phase to the N_X phase, some mesogenic groups suffer angular displacement from the alignment axis. This could be interpreted as a tilt, but a layered structure with a tilt is discounted by x-ray measurements. Another possibility, which we pursue here, is that since the liquid-crystal dimer CB7CB has an odd spacer, many of its conformers will have a bent shape as shown by the molecular field calculations. This is supported by our calculations, to be described shortly, of a negative bend elastic constant for the CB7CB dimer, which becomes more negative with increasing orientational order. As we shall now see, this suggests that a spontaneous twist-bend deformation in the nematic phase might be energetically preferred, rather than the uniform distribution.

Spontaneous symmetry-breaking instabilities in smectic phases of achiral molecules have been identified in a number of systems [57]. These are usually associated with antiferroelectric smectic- C phases. However, Dozov [58] showed that in nematic phases, a negative value for the bend

elastic constant, K_3 , could result in ground-state structures having a nonuniform director distribution instead of the uniform distribution when K_3 is positive. It was found that two deformations are predicted: splay-bend and twist-bend, and the latter is intrinsically chiral. For the splay-bend director deformation, the director, \mathbf{n} , takes the form $(\sin\theta(z), 0, \cos\theta(z))$, where the magnitude of the bend varies along the z axis, which is the unique direction in the problem. The variation of the director orientation along this axis is given by

$$\theta(z) = \theta_0 \sin kz, \tag{7}$$

where k is the wave vector controlling the length scale for the spatial oscillation. The second deformation is the twist-bend deformation, and for this the director has the form $(\sin\theta_0 \cos kz, \sin\theta_0 \sin kz, \cos\theta_0)$. Thus the director is tilted with respect to z , the average director makes a constant angle θ_0 , and also rotates about z . The system is, of course, not chiral and so this helical structure has its equivalent but with the opposite twist. The anticipated molecular organization in the twist-bend director distribution is shown in Fig. 16. The snapshot was taken from a computer simulation of V-shaped molecules formed by linking two Gay-Berne calamitic particles with an interarm angle of 140° [59]. The structure has the anticipated helical organization; the helix axis is vertical and the molecular long axes are tilted more or less uniformly with respect to this. Since the system, overall, is achiral, equal regions of opposite twist are expected but the system size precludes the observation of helices with opposite handedness.

Dozov gives the difference in the elastic free energy between the uniform and the splay-bend deformation as

$$\Delta F_{sb} = K_3^3 / 27 C K_1 \tag{8}$$

and for the twist-bend deformation

$$\Delta F_{tb} = K_3^3 / 54 C K_2. \tag{9}$$

In addition to the three elastic constants, these free-energy differences depend on the factor C , which is a combination of the coefficients for the fourth-order terms, which do not normally appear in the expansion of the elastic free energy. They are needed here in order to provide a bound for the spontaneous bend deformation. Since C is necessarily positive and because K_1 and K_2 are expected to be positive, we see that the free-energy differences will change sign as soon as K_3 passes from positive to negative, leading to a second-order phase transition. The spontaneous stabilization of the splay-bend and twist-bend deformations simply requires a negative value for the bend elastic constant [60]. A recent paper [16] has also suggested that the spontaneously bent nematic phases proposed by Dozov might provide an explanation of the optical textures observed in bis-(phenyl)oxadiazole derivatives.

Unfortunately, the elastic constants for CB7CB have yet to be measured, but as we have seen, it is possible to calculate them with some reliability [44,46]. Accordingly, using the model that accounts so successfully for the magnitude and temperature dependence of the parallel and perpendicular components of the dielectric tensor, we have calculated the three elastic constants for CB7CB. The results for these calculations are shown, in Fig. 17, as a function of the order parameter for the mesogenic groups. It is immediately apparent

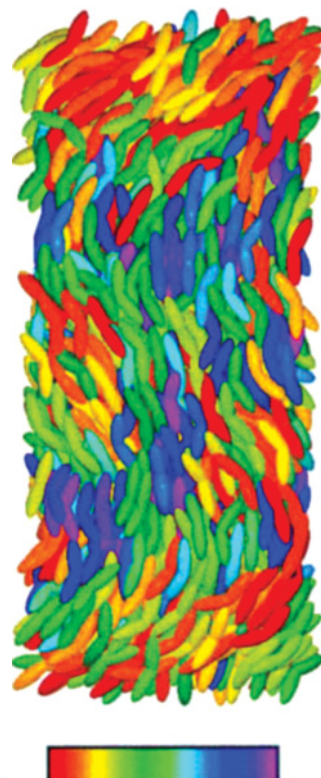


FIG. 16. (Color) A snapshot showing the arrangement of bent or V-shaped molecules in the twist-bend structure. The color code of the molecules indicates the azimuthal angle for the molecular long axis and hence the twist. [Taken with permission from R. Memmer, *Liq. Cryst.* **29**, 483 (2002)].

that the bend elastic constant is indeed negative even when S_{zz} corresponds to that measured at the nematic-isotropic transition. It then decreases dramatically with increasing order. The fact that K_3 is negative over the entire range of measured order parameters should mean that a nematic liquid crystal with a deformed director ground state should appear immediately. Since for CB7CB this deformed state is preceded by a standard nematic liquid crystal, it would seem that the theory tends to overestimate the contribution of bent molecular structures to

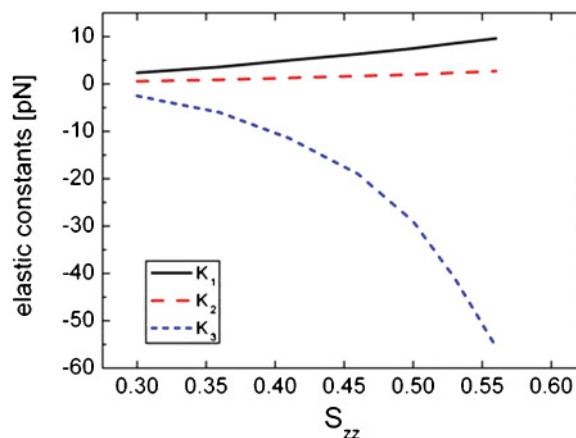


FIG. 17. (Color online) The elastic constants, K_i , calculated for the uniaxial nematic phase of CB7CB as a function of the order parameter, S_{zz} , using the CTP plus SI model.

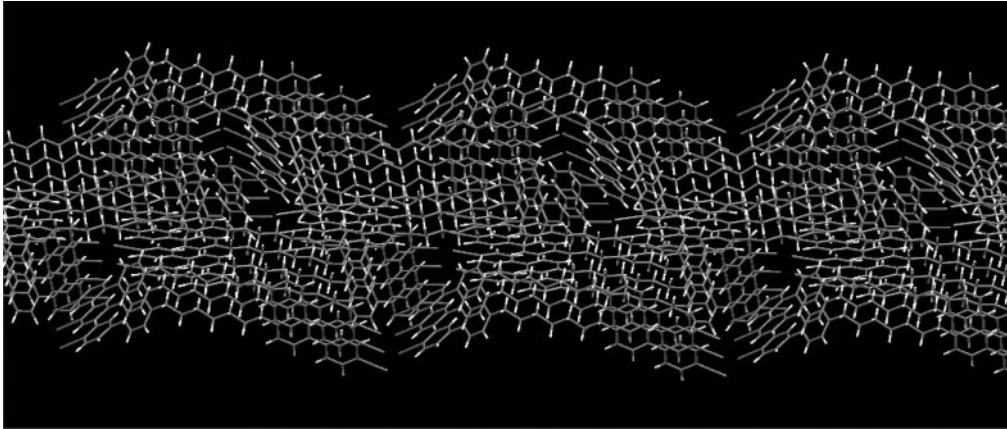


FIG. 18. The crystal structure of CB7CB with the molecules shown as stick models.

the bend elastic constant. Alternatively, there is another elastic contribution that competes with the bend deformation and so prevents the formation of a deformed director ground state.

The relative stability of the two director deformations predicted by Dozov [58] depends on the ratio $K_1/2K_2$. The results for the elastic constants shown in Fig. 17 suggest that this ratio is larger than unity, so that the twist-bend structure should be the ground state. If this is the case, then the chirality needed to make the methylene deuterons inequivalent should be present in the low-temperature nematic phase. In fact, there should be chiral domains occurring in equal amounts but with opposite handedness and equal pitches. There is also an interesting new feature for the liquid-crystal dimer. Unlike the rigid V-shaped molecule considered by Dozov, the dimer is flexible and some of the conformers will be enantiomers. In the standard nematic liquid crystal, these will occur with equal probability so that the phase is achiral. However, in the twist-bend nematic liquid crystal, the chiral nature of the domains could well influence the conformational distribution so that the relative proportions will change and so enhance the chirality of the domains.

While this paper was being prepared, we became aware of the report of experimental observations on liquid-crystal dimers having similar structures to CB7CB, the key feature being the methylene links between the mesogenic groups and the odd spacer [17]. The materials studied had relatively long spacers, namely 1'',11''-bis(4-cyanobiphenyl-4'-yl)undecane, 1'',11''-bis(4-propyl-7,8-di-fluoro-terphenyl-4'-yl)undecane, and 1'',11''-bis(4-pentyl-2',3'-di-fluoro-terphenyl-4'-yl)undecane. The low-temperature nematic phase that they form exhibited optical textures showing periodic deformations in uniform planar aligned samples similar to those in Fig. 2. The authors identified a very weak first-order nematic-nematic phase transition in their materials, accompanied by an identifiable change in optical textures. They propose that the new nematic phase, N_X , supports periodic deformation patterns that, to develop in nematic liquid crystals, require at least K_1 or K_2 to be negative but not K_3 . Significantly, this explanation of the origin of both the stripes and the new nematic phase is at variance with the results of the elastic constant calculations. Indeed, as we

have seen, both K_1 and K_2 are positive and K_3 is negative. It is noteworthy that these materials, in common with that reported in this paper, have terminal mesogenic groups coupled to a flexible chain through methylene links. All of our investigations of flexible dimers having mesogenic groups coupled through oxygen (ether) groups have failed to reveal the presence of any mesogenic phases, other than the simple uniaxial nematic phase. This suggests that the angle made between the mesogenic groups and the linking chain is critical to the local structural organization in the nematic phase N_X . This is quite in keeping with the prediction by Dozov that K_3 needs to be negative to form the new phase and that this elastic constant is sensitive to the bend of the molecule.

The results of our crystal structure determination for CB7CB are given as supplemental material [61] to this paper. They show that in the crystalline state, the molecules are packed in an overlapping fashion with four molecules per unit cell. A representation of the crystal structure is given in Fig. 18, which shows a bend-modulated structure.

The intercalation measured in the crystal phase is consistent with measurements taken from the x-ray scattering images obtained in the liquid-crystalline phases. If the residual bend modulation also persists in the low-temperature liquid-crystal phase, then this would provide an explanation of results reported here for a variety of techniques. However, some caution should be exercised when attempting to infer the liquid-crystal structure from that of the crystal.

Focal conic optical textures are observed for smectic and chiral nematic phases. Their existence depends on the preservation of some optical periodicity, layer spacing for smectic liquid crystals, and helical pitch for chiral nematic liquid crystals. It is conceivable that an optical periodicity associated with a twist-bend nematic liquid crystal would also give rise to the focal conic textures observed for CB7CB.

IX. CONCLUSIONS

The symmetric liquid-crystal dimer CB7CB consists of two cyanobiphenyl groups linked by an alkyl chain of seven methylene groups. It is a molecule of relative simplicity, yet understanding its liquid-crystal phase behavior has proved to

be challenging. We have applied the standard techniques usually employed to explore liquid-crystal phase behavior, and we have established that CB7CB exhibits a normal nematic phase over the range 116–103 °C. At this temperature, it undergoes a weakly first-order transition to a second disordered mesophase, devoid of long-range translational order, identified as a nematic liquid crystal.

Of the experiments carried out on CB7CB in the low-temperature mesophase, the most surprising results were obtained for ^2H NMR, which revealed two major quadrupolar splittings in the N_X phase but just one in the preceding nematic liquid crystal. Deuterium magnetic resonance measurements probe the orientational order with respect to the magnetic field of groups within a mesogen. The observation of two quadrupolar splittings indicates, we believe, that the two deuterons attached to a methylene carbon have lost their equivalence. For this to occur, it is necessary for the phase to be chiral either globally or locally in domains. We believe that the low-temperature mesophase of CB7CB is characterized by a local, probably periodic, bend in the director. Measurements obtained with other techniques can be satisfactorily explained on this basis.

The existence of a bend-modulated nematic phase has been partially supported by theory and calculations, yet many other characteristics of the phase remain to be determined. The phase appears to be relatively viscous, but we have not carried out any viscosity measurements. The phase generates a variety of

optical textures, and furthermore the phase we have designated as a twist-bend nematic phase is expected to be characterized by novel types of defect, but as yet we have not observed these. The twist-bend nematic phase, which has a very small and positive dielectric anisotropy, can be switched from an approximately planar texture to a homeotropic texture by relatively large electric fields. Finally, the unusual nematic phase we have identified in CB7CB should be observable in other molecules of related structure. The requirements for a mesogen to exhibit a twist-bend nematic phase are that there should be at least two mesogenic groups linked by a sufficiently bent geometry to give a negative bend elastic constant.

ACKNOWLEDGMENTS

We are grateful for financial support from The Leverhulme Trust, from the MICINN of Spain (project MAT2009-14636-C03-02, 03), from the Government of the Basque Country (GI/IT-449-10), and the Government of Catalunya (emergent research group AGAUR-2009-SGR-1243). X-ray crystallographic measurements were carried out by Dr. J. B. Orton at the United Kingdom EPSRC National Crystallography Service, University of Southampton. We are grateful to Professor J. W. Emsley, University of Southampton, and Professor P. Lesot, Université de Paris–Sud, for discussions concerning the influence of chirality on deuterium NMR spectra in liquid crystals.

-
- [1] D. Vorländer, *Z. Phys. Chem.* **105**, 211 (1923).
- [2] D. Demus, in *Handbook of Liquid Crystals*, edited by D. Demus, J. W. Goodby, G. W. Gray, H.-W. Speiss, and V. Vill (Wiley VCH, Weinheim, 1998), Vol. 1, Chap. VI, p. 133.
- [3] T. Ganieca and W. Stanczyk, *Materials* **2**, 95 (2009).
- [4] I. M. Saez and J. W. Goodby, *J. Mater. Chem.* **15**, 26 (2005).
- [5] R. Elsässer, G. H. Mehl, J. W. Goodby, and M. Veith, *Angew. Chem. Int. Ed.* **40**, 2688 (2001).
- [6] C. T. Imrie and P. A. Henderson, *Chem. Soc. Rev.* **36**, 2096 (2007).
- [7] C. T. Imrie and G. R. Luckhurst, in *Handbook of Liquid Crystals*, edited by D. Demus, J. W. Goodby, G. W. Gray, H.-W. Speiss, and V. Vill (Wiley VCH, Weinheim, 1998), Vol. **2B**, Chap. X, p. 801.
- [8] G. R. Luckhurst, in *Recent Advances in Liquid Crystalline Polymers*, edited by L. Lawrence Chapoy (Elsevier Applied Science, Barking, UK, 1985), Chap. 7, p. 105; A. Ferrarini, G. R. Luckhurst, P. L. Nordio, and S. J. Roskilly, *J. Chem. Phys.* **100**, 1460 (1994); G. R. Luckhurst and S. Romano, *ibid.* **107**, 2557 (1997).
- [9] D. A. Dunmur, M. R. de la Fuente, M. A. Perez Jubindo, and S. Diez, *Liq. Cryst.* **37**, 723 (2010).
- [10] D. A. Dunmur, G. R. Luckhurst, M. R. de la Fuente, S. Diez, and M. A. Perez Jubindo, *J. Chem. Phys.* **115**, 8681 (2001).
- [11] M. Stocchero, A. Ferrarini, G. J. Moro, D. A. Dunmur, and G. R. Luckhurst, *J. Chem. Phys.* **121**, 8079 (2004).
- [12] G. R. Luckhurst, *Angew. Chem. Int. Ed.* **44**, 2834 (2005).
- [13] M. W. Schroder, S. Diele, G. Pelzl, U. Dunemann, H. Kresse, and W. Weissflog, *J. Mater. Chem.* **13**, 1877 (2003).
- [14] M. Šepelj, A. Lesac, U. Baumeister, S. Diele, H. L. Nguyen, and D. W. Bruce, *J. Mater. Chem.* **17**, 1154 (2007).
- [15] R. A. Reddy and C. Tschierscke, *J. Mater. Chem.* **16**, 907 (2006).
- [16] V. Gortz, C. Southern, N. W. Roberts, H. F. Gleeson, and J. W. Goodby, *Soft Matter* **5**, 463 (2009).
- [17] V. P. Panov, M. Nagaraj, J. K. Vij, Yu. P. Panarin, A. Kohlmeier, M. G. Tamba, R. A. Lewis, and G. H. Mehl, *Phys. Rev. Lett.* **105**, 167801 (2010).
- [18] P. J. Barnes, A. G. Douglass, S. K. Heeks, and G. R. Luckhurst, *Liq. Cryst.* **13**, 603 (1993); P. J. Barnes, Ph.D. thesis, University of Southampton, UK, 1994.
- [19] G. R. Luckhurst, *Liq. Cryst.* **32**, 1335 (2005).
- [20] M. B. Sied, J. Salud, D. O. López, M. Barrio, and J. Tamarit, *Phys. Chem. Chem. Phys.* **4**, 2587 (2002).
- [21] P. Cusmin, M. R. de la Fuente, J. Salud, M. A. Pérez-Jubindo, S. Diez-Berart, and D. O. López, *J. Phys. Chem. B* **111**, 8974 (2007).
- [22] M. A. Pérez-Jubindo, M. R. de la Fuente, S. Diez-Berart, D. O. López, and J. Salud, *J. Phys. Chem. B* **112**, 6567 (2008).
- [23] J. Thoen, G. Cordoyiannis, and C. Glorieux, *Liq. Cryst.* **36**, 669 (2009).
- [24] C. W. Garland and M. E. Huster, *Phys. Rev. A* **35**, 2365 (1987).
- [25] X. Wen, C. W. Garland, and M. D. Wand, *Phys. Rev. A* **42**, 6087 (1990).
- [26] S. Diez, Doctoral thesis, University of the Basque Country, Bilbao, 2003.
- [27] D. Bauman, E. Wolarz, and E. Bialecka-Florjanczyk, *Liq. Cryst.* **26**, 45 (1999).

- [28] A. Ferrarini, G. R. Luckhurst, P. L. Nordio, and S. J. Roskilly, *Chem. Phys. Lett.* **214**, 409 (1993).
- [29] A. Ferrarini, G. R. Luckhurst, P. L. Nordio, and S. J. Roskilly, *Liq. Cryst.* **21**, 373 (1996).
- [30] G. R. Luckhurst, M. Setaka, and C. Zannoni, *Mol. Phys.* **28**, 49 (1974).
- [31] F. S. M. Chui, C. T. Imrie, and G. R. Luckhurst (in preparation).
- [32] H. Toriumi (unpublished).
- [33] A. Kumar, P. K. Karahaliou, A. G. Vanakaras, and D. J. Photinos, Abstract P6-05, 11th ECLC (to be published, 2011).
- [34] D. Merlet, A. Loewenstein, W. Smadja, J. Courtieu, and P. Lesot, *J. Am. Chem. Soc.* **120**, 963 (1998).
- [35] C. Aroulanda, D. Merlet, J. Courtieu, and P. Lesot, *J. Am. Chem. Soc.* **123**, 12059 (2001).
- [36] J. W. Emsley, R. Hashim, G. R. Luckhurst, and G. N. Shilstone, *Liq. Cryst.* **1**, 437 (1986).
- [37] J. W. Emsley, P. Lesot, J. Courtieu, and D. Merlet, *Phys. Chem. Chem. Phys.* **6**, 5331 (2004).
- [38] J. W. Emsley, G. R. Luckhurst, and G. N. Shilstone, *Mol. Phys.* **53**, 1023 (1984).
- [39] A. Ferrarini, G. J. Moro, P. L. Nordio, and G. R. Luckhurst, *Mol. Phys.* **77**, 1 (1992).
- [40] G. R. Luckhurst, C. Zannoni, P. L. Nordio, and U. Segre, *Mol. Phys.* **30**, 1345 (1975).
- [41] P. J. Flory, *Statistical Mechanics of Chain Molecules* (Interscience, New York, 1969).
- [42] A. Ferrarini, G. R. Luckhurst, and P. L. Nordio, *Mol. Phys.* **85**, 131 (1995).
- [43] M. J. Frisch *et al.*, *Gaussian 03 Revision C.02* (Gaussian Inc., Wallingford, CT, 2004).
- [44] M. Cestari, Doctoral thesis, University of Padua, 2008.
- [45] A. Ferrarini, C. Greco, and G. R. Luckhurst, *J. Mater. Chem.* **17**, 1039 (2007).
- [46] M. Cestari, A. Bosco, and A. Ferrarini, *J. Chem. Phys.* **131**, 054104 (2009).
- [47] B. Kundu, R. Pratibha, and N. V. Madhusudana, *Phys. Rev. Lett.* **99**, 247802 (2007).
- [48] G. R. Luckhurst, *Thin Solid Films* **393**, 40 (2001).
- [49] M. Petrov, A. Braslau, A. M. Levelut, and G. Durand, *J. Phys. II* **2**, 1159 (1992).
- [50] S. V. Vasilenko, A. R. Khokhlov, and V. P. Shibaev, *Macromolecules* **17**, 2270 (1984).
- [51] G. Ungar, V. Percec, and M. Zuber, *Macromolecules* **25**, 75 (1992).
- [52] G. Ungar, V. Percec, and M. Zuber, *Polymer Bull.* **32**, 325 (1994).
- [53] S. R. Warriar, D. Vijayaraghavan, and N. V. Madhusudana, *Europhys. Lett.* **44**, 296 (1998).
- [54] B. Kundu, S. K. Pal, S. Kumar, R. Pratibha, and N. V. Madhusudana, *Europhys. Lett.* **85**, 36002 (2009).
- [55] A. Eremin, A. Nemes, R. Stannarius, G. Pelzl, and W. Weissflog, *Soft Matter* **4**, 2186 (2008).
- [56] M. G. Tamba, U. Baumeister, G. Pelzl, and W. Weissflog, *Liq. Cryst.* **37**, 853 (2010).
- [57] D. R. Link, G. Natale, R. Shao, J. E. Maclennan, N. A. Clark, E. Körblova, and D. M. Walba, *Science*, **278**, 1924 (1997).
- [58] I. Dozov, *Europhys. Lett.* **56**, 247 (2001).
- [59] R. Memmer, *Liq. Cryst.* **29**, 483 (2002).
- [60] We have named these two new nematic phases according to their differing director distributions as splay-bend and twist-bend nematic liquid crystals to recall the nature of the director deformation. This is in keeping with the name used for the nematic liquid crystal with a helically twisted director as a chiral nematic phase.
- [61] See Supplemental Material at <http://link.aps.org/supplemental/10.1103/PhysRevE.84.031704> for details of the x-ray crystal structure determination of CB7CB, and also for modulated differential scanning calorimetry measurements made in the region of the isotropic-to-nematic phase transition for CB7CB.